Biomedicine & Pharmacotherapy 145 (2022) 112464

Contents lists available at ScienceDirect

Biomedicine & Pharmacotherapy

journal homepage: www.elsevier.com/locate/biopha

Photodynamic therapy with the dual-mode association of IR780 to PEG-PLA nanocapsules and the effects on human breast cancer cells

Marina Guimarães Carvalho Machado, Maria Alice de Oliveira, Elisa Gomes Lanna, Raoni Pais Siqueira, Gwenaelle Pound-Lana, Renata Tupinambá Branquinho, Vanessa Carla Furtado Mosqueira [*,1]

Laboratory of Pharmaceutics and Nanotechnology, School of Pharmacy, Federal University of Ouro Preto, Minas Gerais, Brazil

ARTICLE INFO

Keywords:
Phototheranostics
IR780
Polymeric nanocapsules
Image-guided therapy
Photodynamic therapy
Polymer conjugation

ABSTRACT

IR780 is a near-infrared fluorescent dye, which can be applied as a photosensitizer in photodynamic (PDT) and photothermal (PTT) therapies and as a biodistribution tracer in imaging techniques. We investigated the growth and migration inhibition and mechanism of death of breast tumor cells, MCF-7 and MDA-MB-231, exposed to polymeric nanocapsules (NC) comprising IR780 covalently linked to the biodegradable polymer PLA (IR-PLA) and IR780 physically encapsulated (IR780-NC) *in vitro*. Both types of NC had mean diameters around 120 nm and zeta potentials around −40 mV. IR-PLA-NC was less cytotoxic than IR780 NC to a non-tumorigenic mammary epithelial cell line, MCF-10A, which is an important aspect of selectivity. Free-IR780 was more cytotoxic than IR-PLA-NC for MCF-7 and MDA-MB-231 cells after illumination with a 808 nm laser. IR-PLA NC was effective to inhibit colony formation (50%) and migration (30–40%) for both cancer cell lines. MDA-MB-231 cells were less sensitive to all IR780 formulations compared to MCF-7 cells. Cell uptake was higher with IR-PLA-NC than with IR780-NC and free-IR780 in both cancer cell lines ($p < 0.05$). NC uptake was higher in MCF-7 than in MDA-MB-231 cells. IR-PLA-NC induced a higher percentage of apoptosis upon illumination in MDA-MB-231 than in MCF-7 cells. The necrosis mechanism of death predominated in treatments with free-IR780 and with encapsulated IR780 NC, suggestive of damages at the plasma membrane. IR780 conjugated with PLA increased the apoptotic pathway and demonstrated potential as a multifunctional theranostic agent for breast cancer treatment with increased cellular uptake, photodynamic activity and more reliable tracking in cell-image studies.

1. Introduction

Cancer is the second leading cause of death in the world and was responsible for 9.6 million deaths in 2018, according to the Pan American Health Organization (PAHO). Cancer mortality in the Americas is projected to increase to 2.1 million by 2030 [1] According to the National Cancer Institute (INCA/Brazil), breast cancer is the most common type of cancer among women in the world and in Brazil, accounting for about 66,280 new cases in Brazil in 2010, which corresponds to 29.7% of the total number of neoplasms [2].

Conventional chemotherapy in clinical use frequently fails to completely eradicate tumors and induces severe side effects. The lack of selectivity and high toxicity of antitumor drugs, and multidrug resistance limit their therapeutic efficacy [3]. Phototherapies are in advanced clinical trials, including photodynamic therapy (PDT) and photothermal therapy (PTT) for some types of cancer. The Food and Drug Administration (FDA) have already approved this therapeutic approach in the United States for the treatment of obstructive esophageal cancer [4].

The use of nanotechnology for the treatment of tumors has been extensively studied to increase drug concentrations at the tumor site, selectively destroying cancer cells and dramatically decreasing the side effects on healthy cells. Several FDA-approved nanomedicines are currently in clinical use to treat various types of cancer and many others are in clinical development [5]. However, some challenges remain, including how to monitor the biodistribution and control off-target

* Correspondence to: Laboratório de Desenvolvimento Galênico e Nanotecnologia, Escola de Farmácia, Universidade Federal de Ouro Preto, Campus Morro do Cruzeiro, Ouro Preto, Minas Gerais 35400-000, Brazil.
E-mail address: mosqueira@ufop.edu.br (V.C.F. Mosqueira).
[1] ORCID: 0000-0002-0368-6090.

https://doi.org/10.1016/j.biopha.2021.112464
Received 31 August 2021; Received in revised form 16 November 2021; Accepted 19 November 2021
Available online 1 December 2021

effects of drugs and bioactive compounds. In nanomedicine-based theranostics the same nanocarrier has the ability to monitor tumor cells by imaging techniques, and destroy the cells, allowing for non-invasive detection and more accurate chemotherapy [3].

In addition, one of the challenges of nanotechnology is the development of nanoparticles with multiple functions. IR780, a photosensitizer (PS) and fluorescent probe, is known to preferentially accumulate in the mitochondria of tumor cells [6]. IR780 entry into cells seems to be mediated by the organic anion-transporting polypeptide (OATP) superfamily transporters expressed in various types of tumors with poor prognosis [7]. Many studies showed a high degree of co-localization of IR780 and Mito-tracker confirming their targeting to mitochondria [8]. The mechanism of cell death suggested for IR780 is based on the generation of reactive oxygen species (ROS) upon illumination with a laser that can be modulated to induce cell apoptosis [9]. ROS may cause substantial harm to tumors and stimulate the immune system's anticancer activity [5]. The oxidative damage can occur via three main pathways: apoptosis, necrosis or autophagy [10]. ROS can lead to the oxidation of cellular constituents such as proteins, lipids or DNA [11]. IR780 uptake and delivery is directly related to cell death. Furthermore, IR780 exhibits outstanding photophysical properties as a near-infrared (NIR) emission probe and can be used in imaging techniques as a tumor tracer agent [12]. In this sense, IR780 is a promising molecule to be applied in PDT and PTT as a photosensitizer (PS) due to its versatility.

However, IR780 has low water solubility, fast plasma clearance, poor stability in aqueous media, and shows acute toxicity at high doses (1 mg/kg in mice), which limit its clinical application [13]. The literature reports IR780 loaded in different types of nanostructures, which have improved its pharmacokinetics and pharmacodynamics properties. It is worth noting that most studies used IR780 physically encapsulated in nanostructures as a tracer agent without a detailed demonstration of the stability of IR780 loading [14-17]. Few studies using IR780 conjugates are reported in the literature. Yuan et al. [18] developed a self-assembled micellar system based on C13 alkyl chain linked to IR780 and PEG. Nonetheless, micelles are less stable than polymeric nanoparticles upon dilution [19,20]. Other studies conjugated IR780 with hyaluronic acid [13] or with abiraterone [9]. Transfer of IR780 from the different types of nanostructures or disassembly of micelles upon dilution in biological media were not investigated in the majority of the studies involving nanocarriers.

In order to ensure that IR780 provides stable labeling of nanoparticles and would be firmly attached to the nanoparticle to reach the tumor site at an appropriate concentration, in our recent study, we covalently linked IR780 to poly(*D,L*-lactide) (PLA), represented in (Fig. 1) as IR-PLA [21]. This polymer-dye conjugate can be applied in imaging studies *in vivo* (biodistribution), where the nanoparticle and the fluorescent dye will be co-located, warranting real monitoring of the particles and of the photosensitizer. Additionally, flow field-flow fractionation (AF4) analyses of IR780 loaded nanospheres (NS) containing IR-PLA or IR780 showed that there was a transfer of about 50% of the initial fluorescence of IR780 from the NS to the serum proteins present in the incubation medium within 16 h when the dye was physically encapsulated [22]. In contrast, IR-PLA NS exhibited negligible transfer of fluorescence to the proteins [22] In a previous work we reported the effects of serum protein on NP uptake of IR-780 associated to NC by murine macrophages in a proof-of-concept approach [23]. These results highlighted the importance of covalently binding the fluorophore to the polymer for reliable tracking of nanoparticles in cells and tissues.

In this study we investigate the main mechanisms of cell death in MCF-7 and MDA-MB-231 breast tumor cell lines, and the effects on cell growth and migration inhibition exposed to polymeric nanocapsules (NC) containing IR780 *in vitro*. The photodynamic activity of the formulations was estimated under photo-illumination with 808 nm laser. Throughout the study we compare the dual-mode of association of IR780 to the NC, i.e. IR780 physical encapsulation (IR780-NC) vs covalent bond to the biodegradable polymer PLA (IR-PLA). PEG-PLA nanocapsules were prepared by co-precipitation of PEG-PLA and IR-PLA, as shown in Fig. 1, so that all NC are sterically stabilized by a PEG corona. Selectivity was estimated from cytotoxicity toward the non-tumorigenic mammary epithelial human breast cell line MCF-10A.

2. Materials and methods

2.1. Materials

The fluorescent dye IR780, iodide (2-[2-[2-chloro-3-[(1,3- dihydro-3,3-dimethyl-1-propyl-2H-indol-2-ylidene)ethylidene]-1-cyclohexen-1-yl]ethenyl]-3,3-dimethyl- 1-propylindolium iodide) was provided by Sigma-Aldrich Co (St. Louis, MO, USA). The polymers used in NC preparation were monomethoxy-polyethylene glycol-*block*-polylactide (PEG_{5k}-PLA_{20k}, Mn = 22,200 g/mol, Đ = 1.38) and *D,L*-polylactide (PLA_{20k}) synthesized and characterized according to methodology described in Pound-Lana et al. [24]. The IR780-polymer conjugates (IR-PLA, Mn = 4000 g/mol, Đ = 1.26) were synthesized and characterized as described [21]. Acetone and methanol (PA grade) were obtained from Vetec (RJ, Brazil), Miglyol®810N (triglyceride of caprylic (C8)/capric (C10) acids) from Sasol (Gmbh, Germany), and lecithin (Lipoid®S75 with approximately 75% phosphatidylcholine) were acquired from Lipoid (Gmbh, Germany). Ultrapure water was obtained on a Simplicity-MilliQ system (Millipore, USA). The phosphate-buffered saline (PBS) and Dulbecco's Modified Eagle Medium (DMEM, 4.5-g/L glucose and L-glutamine) media, trypsin-EDTA (0.25%) and antibiotic stock solution (10,000 IU of penicillin + 10 mg/mL of streptomycin) were provided by Lonza (USA) and inactivated fetal bovine serum (FBS) was acquired from Cultilab (Brazil). DMEM/HAM F12 medium and

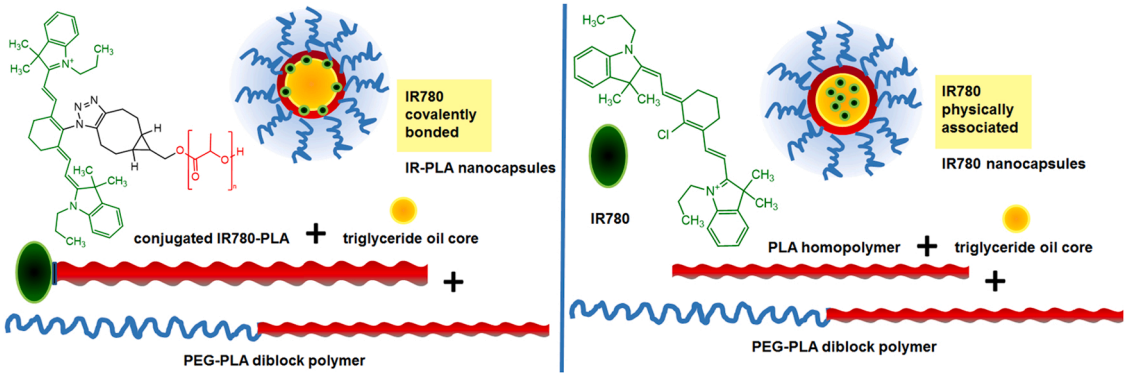

Fig. 1. A schematic representation of PLA-PEG nanocapsules containing the fluorescent probe IR780 covalently bound to poly(*D,L*-lactide) (IR-PLA) or physically associated (IR780 NC).

DMEM/F-12 medium without phenol red were acquired from GE Healthcare Life Sciences HyClone (Utah, USA). Roswell Park Memorial Institute (RPMI) medium 1640 with L-glutamine and the MTT reagent, 3-(4,5-dimethylthiazol-2-yl)-2,5-diphenyltetrazolium bromide, were provided by Gibco® Life Technologies (Carlsbad, USA) and dimethyl sulfoxide (DMSO) acquired from Synth (RJ, Brazil).

2.2. Synthesis of IR-PLA

IR-PLA was synthesized via one-pot strain-promoted azide-alkyne cycloaddition, according to the methodology described by Oliveira et al. [21]. Briefly, cyclooctyne endfunctional polylactide (BCN-PLA_{4k}, 50 mg; 1.25×10^{-5} mol), IR780 (4.17 mg; 6.25×10^{-6} mol) and sodium azide (4.06 mg; 6.25×10^{-5} mol) were solubilized in dry DMF (5 mL). The reaction was allowed to proceed protected from light for 16 h at 25 °C, under magnetic stirring and in an argon atmosphere. The solvent was removed under reduced pressure. The product was solubilized in ethyl acetate (10 mL) and centrifuged for 5 min at 500×*g* for the removal of salts (residual sodium azide and sodium chloride). The supernatant was collected, the solvent was evaporated under high vacuum and the product was IR-PLA with one IR780 covalently bound at one chain-end and molar mass and dispersity by GPC of 4000 g/mol and 1.26, respectively.

2.3. Preparation of nanocapsules and IR780 quantification

Polymeric NC were prepared as previously reported [23]. Briefly, to prepare blank-NC (NC without IR780) 24 mg of the polymer PEG-PLA and 5 mg of PLA were dissolved in 8 mL of acetone with 30 mg of lecithin and 100 μL of Miglyol® 810N at 40 °C. After complete dissolution, this organic phase was poured via a syringe into 16 mL of ultrapure water and kept under magnetic stirring at 25 °C for 10 min. Then the solvents (all acetone and water) were evaporated under reduced pressure at 35 °C until a final volume of 4 mL. In order to produce IR780 loaded NC by physical encapsulation (named IR780-NC), an aliquot of stock solution of IR780 in ethanol was placed into the organic phase (containing PEG-PLA, PLA, lecithin and Miglyol® 810N) before mixing with water to obtain a concentration of 27 μg/mL of the dye. To prepare IR-PLA NC (IR780 covalently linked to PLA), 5 mg of PLA were substituted by 5 mg of IR-PLA in the same procedure as for blank-NC formulation. The total amount of IR780 in the NC as well as the non-encapsulated IR780, present in the dispersion (free IR780) was determined by the ultrafiltration-centrifugation method and IR780 quantified by HPLC-UV [23]. The encapsulation efficiency (%) (EE) was determined using the following equation:

$$EE\% = \frac{\text{Total IR780 in NC dispersion} - \text{IR780 in ultrafiltrate} \times 100}{\text{Total IR780 fed in the formulation}}$$

2.4. Nanocapsule characterization

The average hydrodynamic diameters (Dh) and polydispersity indices (PdI) were determined by dynamic light scattering (DLS) on a Zetasizer Nano ZS (Malvern Instrument, UK) instrument equipped with a 633-nm He-Ne laser, at 173° scattering angle. Zeta potentials were determined by electrophoretic laser Doppler anemometry on the same equipment. Nanoparticle dispersions were diluted 5:1000 in ultrapure water and 1 mM NaCl, in appropriate cuvettes to measure sizes and zeta potentials, respectively. Analyses were performed at 25 °C in three different batches of each formulation and in triplicate on each sample.

2.5. Cell culture

The breast cancer cell lines MCF-7 (ATCC® HTB-22), MDA-MB-231 (ATCC® HTB-26) and non-tumorigenic mammary epithelial cell line MCF-10A (ATCC® CRL-10317) were supplied by Cell Bank of Rio de Janeiro (BCRJ). MCF-7 cells were maintained in RPMI medium supplemented with 20% (v/v) FBS and 1% (v/v) penicillin/streptomycin. MDA-MB-231 were cultured in Dulbecco's Modified Eagle Medium (DMEM, 4.5 g/L glucose and L-Glutamine) supplemented with 10% (v/v) FBS and 1% penicillin/streptomycin. MCF-10A cells were maintained in DMEM/HAM F12 medium supplemented with 5% (v/v) heat-inactivated horse serum, 0.01% cholera toxin, 10 μg/mL insulin, 0.1% EGF, 0.05% hydrocortisone and 1% penicillin/streptomycin. The cells were maintained at 37 °C in an incubator humidified and saturated with 5% CO_2. For experiments, cells were detached with trypsin-EDTA (0.25%) from 75 cm^2 bottles and counted using trypan blue exclusion assay in a Neubauer chamber.

2.6. Cell viability

MCF-7 and MDA-MB-231 were seeded at a density of 2.4×10^4 cells/well; and MCF-10A at 6.0×10^3 cells/well, for 24 h of treatment; and 1.2×10^4 cells/well for MCF-7 and MDA-MB-231, for 48 h of treatment, in 96-well plates and incubated at 37ºC under an atmosphere of 5% CO_2 for 24 h for adherence in the respective culture media mentioned above. Then, the culture medium was removed and 200 μL of fresh medium containing blank-NC, IR780-NC, IR-PLA NC or free-IR780 solution in different concentrations of IR780 were added. For each dilution, aliquots of the suspension were placed in triplicate and the experiment repeated twice (n = 6). After incubation, the medium containing the treatment was removed, the wells were washed 3 times with PBS with Ca^{2+} and Mg^{2+}, and then 200 μL of MTT (0.5 mg/mL in culture medium) was added and incubated for another 4 h [25]. After the incubation time, the plates were centrifuged at 600 ×*g* for 5 min, the medium was carefully removed and 200 μL of DMSO was added to each well. To ensure complete dissolution of the formazan crystals, the plates were left in the oven for 15 min and then mixed on a plate shaker for 5 min. Finally, absorbance measurements were performed by spectrophotometry at a wavelength of 570 nm in a Microplate Reader Emax (Molecular Devices Emax). Untreated cells were used as controls, corresponding to 100% of cell viability. CC_{50} (concentration of nanoparticles that are cytotoxic for 50% of cells) were calculated from the viability % versus concentration curve using GraphPad Prism® version 6.01 program.

2.7. Photodynamic toxicity of IR780 nanocapsules in vitro

Cell suspensions were seeded in 96-well plates, leaving one column space and one cell-free row between the wells, at densities of 2.4×10^4 cells/well for MCF-7 and MDA-MB-231 and incubated at 37ºC under a 5% CO_2 atmosphere for 24 h for adherence in the respective culture media. Then, the culture medium was removed and substituted by 200 μL of fresh culture medium containing blank-NC, IR-PLA NC, IR780 NC or free-IR780 (0.8 and 1.6 μg/mL of IR780). Each dilution was performed in triplicate. After 2 h of treatment, the medium was removed, the wells were washed twice with PBS with Ca^{2+} and Mg^{2+}. Then 200 μL of DMEM without phenol red and FBS were added. Each well was then illuminated with a laser at 808 nm (1 W/cm^2) for 5 min using a laser probe (Therapy EC laser equipment, DMC equipment, Brazil). The medium was replaced with DMEM or RPMI supplemented with FBS according to each cell line and the plates were incubated for another 24 h. At the end of the incubation time, the cell viability was quantified by the MTT test, as described in Section 2.6. Plates treated identically but not illuminated with laser were used as controls. Cell viability was defined as the percentage of surviving cells compared to untreated control cells.

2.8. Quantitative determination of reactive oxygen species (ROS) by flow cytometry

The production of ROS was quantified using 2,7-dichlorofluorescein

diacetate (DCFH-DA). MCF-7 and MDA-MB-231 cells were seeded at a density of 5×10^5 cells/well placed in 12-well plates and incubated at 37 °C under 5% CO_2 atmosphere for 24 h. Then, the medium was replaced with 1 mL of fresh culture medium containing the treatment: IR780 NC, IR-PLA NC or free-IR780 (1.6 μg/mL of IR780) and the plates were further incubated for 50 min at 37 °C under 5% CO_2 atmosphere. $\cdot H_2O_2$ (2 M) was used as positive control. After washing once with PBS with Ca^{2+} and Mg^{2+}, the cells were incubated with 500 μL of DCFH-DA (25 mM) for 15 min. Subsequently, the cells were washed with PBS and 500 μL of DMEM without phenol red and FBS was added. Each well was illuminated with a laser at 808 nm (1 W/cm^2) for 5 min using Therapy EC laser equipment (DMC equipment, Brazil). The cells were detached with 300 μL of trypsin-EDTA (0.25%) in each well with a 5 min incubation time. Trypsin was neutralized with 300 μL of culture medium and the contents of each well were transferred to Eppendorf tubes and taken for centrifugation at 500×*g* for 5 min. Cells were washed with PBS with Ca^{2+} and Mg^{2+} and centrifuged three times. Finally, the cells were resuspended in 500 μL of PBS in cytometer tubes, and analyzed in FACSCalibur flow cytometer (Becton Dickinson, USA), where 25,000 events per analysis were acquired. Green fluorescence was collected on the FL1 channel for intracellular DCFH. The results were analyzed using Flow Jo software (Becton Dickinson). Cells labeled with DCFH, without treatment were used as controls and the basal ROS production was normalized as 1.

2.9. Apoptosis analysis by flow cytometry

The Annexin V-FITC Apoptosis Detection Kit I (BD Biosciences) was used to determine the effects of treatment on breast cancer cell apoptosis. MDA-MB-231 and MCF-7 cells were plated at a density of 5×10^5 cells/well in 12-well plates and incubated at 37ºC under 5% CO_2 atmosphere for 24 h. Then, the culture medium was replaced by medium containing the treatment, i.e. IR780 NC, IR-PLA NC and free-IR780 (3.2 μg/mL of IR780) and the plates were incubated for 2 h. The medium was removed, the wells were washed twice with PBS with Ca^{2+} and Mg^{2+} and then 500 μL of DMEM without phenol red and FBS were added. Each well was illuminated with a laser at 808 nm (1 W/cm^2) for 5 min using Therapy EC laser equipment (DMC equipment, Brazil). The medium was then replaced with DMEM or RPMI supplemented with FBS according to each cell line and the plates were incubated for another 24 h. After treatment, the culture medium was removed, the cells were washed with PBS with Ca^{2+} and Mg^{2+} three times, and 300 μL of trypsin-EDTA (0.25%) was added to each well. The plate was left in the oven for 5 min, and trypsin was neutralized with 300 μL of culture medium. The contents of each well were transferred by pipette to Eppendorff tubes and taken for centrifugation at 500×*g* for 5 min. The cells were washed with PBS with Ca^{2+} and Mg^{2+} three times. After the last centrifugation, 100 μL of the cell suspension were transferred to a cytometer tube and labeled according to the manufacturer's protocol. The tubes were taken immediately for analysis in FACSCalibur flow cytometer (Becton Dickinson, USA), where 25,000 events were acquired per analysis. The results were analyzed using Flow Jo software (Becton Dickinson). Annexin V–FITC+/PI- cells were considered early apoptotic cells, annexin V–FITC+/PI+ cells were considered late apoptotic cells, annexin V–FITC-/PI- are live cells and annexin V–FITC-/PI+ are necrotic cells.

2.10. Clonogenic assay

The ability of NC formulations to inhibit colony formation was evaluated according to the assay previously described [26]. MCF-7 and MDA-MB-231 cells were plated in 6-well plates at a density of 1×10^3 cells/well in a total volume of 3 mL of culture medium per well. They were incubated at 37ºC under an atmosphere of 5% CO_2 for 24 h for adherence, and the culture medium was removed to add 3 mL of fresh culture medium containing blank-NC, IR-PLA NC, IR780 NC or free-IR780 solution (0.8 and 1.6 μg/mL). After 24 h the medium was removed and the wells washed twice with PBS. Culture medium was added to each well (3 mL) and replaced every 3 days for 2 weeks. After 2 weeks, when the number of control colonies had already increased, the assay was terminated. The culture medium was removed, the wells washed twice with PBS and the cells were fixed with 500 μL of 4% formaldehyde for 20 min. After removing the formaldehyde solution, 500 μL of methanol were added for cell hydration and the plate was incubated for another 20 min. Finally, the cells were stained with 500 μL of crystal violet (0.5% in methanol) at room temperature for 5 min, carefully washed with distilled water and the plates were allowed to dry at room temperature. After analysis by microscopy, 600 μL of 33% acetic acid was added for 2 min and 100 μL of the solution was removed and transferred to a 96-well plate for absorbance reading in an ELISA plate reader (Molecular Devices Emax) at 570 nm. The total experiment was carried out twice. The determination of colony formation was calculated by comparing the number of colonies in the control wells (not subjected to treatment, considered as 100%) and in the treated wells.

2.11. Scratch wound assay

To assess the migration capacity of the cells under study after treatment with the formulations, MCF-7 and MDA-MB-231 cells were seeded at a density of 2×10^5 cells/well in 12-well plates in 1 mL of culture medium [27,28]. The plates were incubated at 37 °C under 5% CO_2 atmosphere until the cells reached about 80–90% confluence. The culture medium was removed and a scratched area was created using a sterile 200 μL pipette tip into each well. The plate wells were then visualized under an inverted microscope Axio-Vert (Zeiss, Germany), where photos of three fields/well were recorded at a magnification of 20 x, considered as the initial time. The wells were washed with PBS and new culture medium was added with blank-NC, IR-PLA NC, IR780 NC or free-IR780 (1.6 μg/mL of IR780). Treatment was removed after 24 h and the wells were washed twice with PBS. Cell migration to the scratched surface was analyzed using ImageJ software, where the percentage of inhibition of cell migration was calculated by comparing the initial and post-treatment cell-free area.

2.12. Confocal laser scanning fluorescence microscopy

Microscopy analysis of semi-qualitative uptake of the different formulations were performed using confocal laser scanning fluorescence microscope LSM 780 (Zeiss, Germany). Two human breast cancer cell lines were used, MCF-7 and MDA-MB-231. The cell suspensions were seeded in 24-well plates at a density of 1×10^5 cells/well, containing sterile round coverslips at the bottom of the wells. The plates were incubated for 24 h at 37ºC under a 5% CO_2 atmosphere. After 24 h, the culture medium was replaced by 1000 μL of fresh medium containing the treatment (blank-NC, IR-PLA NC, IR780 NC and free-IR780) or pure culture medium for the control cells. The plates were incubated for another 2 h. The treatment was removed and the wells were washed 3 times with PBS. The cells were fixed using 300 μL/well of a 10% formaldehyde aqueous solution for 20 min and washed with PBS. Then, nuclear DNA was labeled with 200 μL of DAPI solution (0.1 μg/mL in PBS) for 20 min at room temperature, and the wells were washed with PBS. The coverslips were mounted on glass slides and the cell observed under confocal microscopy. The excitation wavelength was 358 nm and 633 nm for DAPI and IR780, respectively. The images were processed in Zen pro 2012 software.

2.13. Quantitative cell uptake by flow cytometry

Quantitative studies of cell uptake of the different formulations were performed in a BD FORTESSA flow cytometer (Becton Dickinson, USA). Cell-associated fluorescence was quantified in MCF-7 and MDA-MB-231 cells at a density of 5×10^5 cells/well seeded in 12-well plates and incubated at 37°C under a 5% CO_2 atmosphere for 24 h for adherence.

The culture medium was removed and 1 mL of fresh medium containing IR-PLA NC, IR780 NC or free-IR780 at specific concentrations were added. For dose-dependent studies, different concentrations of IR780 (0.2, 0.4, 0.8, 1.6, 2.4 and 3.2 μg/mL) were used and the cells were incubated for 2 h at 37 °C. Furthermore, cells were incubated with IR-PLA NC, IR780 NC or free-IR780 at 1.6 μg/mL for different time periods (1, 2, and 4 h) for time-dependent study. Treatment was removed at the end of the treatment time and the wells washed with PBS twice. Then, trypsin (300 μL) was added to each well, left for 2 min, and it was neutralized with 300 μL of culture medium. The cell suspensions were transferred to Eppendorf tubes, centrifuged at 500 × *g* for 5 min, and the cell pellet was washed 3 times with PBS. Finally, the cells were suspended in 300 μL of PBS in the cytometer tubes, which were immediately analyzed in a BD LSR Fortessa TM flow cytometer (Becton Dickinson, USA). The analysis of the fluorescence intensity in the cells was acquired in 50,000 total events after excitation with the red laser (633 nm), on the same reading channel as the APC-Cy7 fluorochrome (filter 780/60) [29,30,17,31]. Results were analyzed using FlowJo software (Becton Dickinson, USA).

2.14. Statistical analysis

Data were analyzed using GraphPad Prism® software version 6.01 (San Diego, CA) and expressed as mean ± standard deviation. Size distributions and zeta potential were analyzed by ANOVA (Tukey's test). The cell culture experiments were performed in triplicate and the experiment repeated twice (n = 6). Unpaired student's *t*-test and one-way ANOVA test followed by Tukey's test were used for cell study analyses. Other specific statistical tests are stated in the figure legends. Statistical significance was set at $p < 0.05$.

3. Results

3.1. Preparation and physicochemical characterization of nanocapsules

IR-PLA polymer was characterized as previously described [21]. A polymer of 4 $kg.mol^{-1}$ molar mass was obtained with 21.6 μg of IR780/mg of IR-PLA polymer. Three types of NC were prepared: blank-NC (containing PEG-PLA and PLA, without IR780), IR780 NC (containing PEG-PLA and PLA, and IR780 encapsulated) and IR-PLA NC (containing PEG-PLA and IR covalently bound to PLA, IR-PLA), as shown in Fig. 1. The three NC formulations (blank-NC, IR780 NC and IR-PLA NC) presented similar average size distributions with no significant differences in the hydrodynamic diameters determined by DLS. They were narrow monodispersed particle populations with PdI values below 0.172 (Table 1).

Zeta potential values were all negative (around −40 mV) and show an electrically stabilized surface that maintains electrostatic repulsion between particles in the aqueous dispersion. These results are consistent with previously described polymeric NC containing IR-PLA and encapsulated IR780 [23]. There were no significant differences in the zeta potential values determined under our experimental conditions.

Table 1
Physicochemical characterization of nanocapsule[a] formulations.

NC	Mean D_h ± SD (nm)	PdI	Zeta potential ± SD (mV)	EE (%)
Blank-NC	118.7 ± 0.5	0.166	-41.5 ± 1.6	–
IR780 NC	122.2 ± 0.4	0.163	-41.7 ± 0.2	95
IR-PLA NC	118.6 ± 1.1	0.172	-37.3 ± 0.5	99

D_h: hydrodynamic diameter; SD: standard deviation (n = 3); PdI: polydispersity index, EE: encapsulation efficiency.

[a] IR780 physically loaded (IR780 NC), covalently linked do PLA (IR-PLA NC) and nanocapsules without IR780 (blank-NC).

3.2. Cell viability

We selected IR780 concentrations for our cell viability studies based on our previous data [23] and according to reported data from other authors [17,32]. The viability results of three cell lines exposed to increasing concentrations of polymers (52.5–1680 μg/mL) and IR780 (0.2–6.4 μg/mL) in NC formulations in 24 and 48 h incubation time are shown in Fig. 2.

The blank-NC induce no significant cytotoxicity for all types of breast cells. Cell viability was reduced only from polymer concentrations of 600 μg/mL and they were not able to decrease the cell viability below 50% even at the highest concentration tested at 24 and 48 h of incubation. MDA-MB-231 cells were less sensitive to the NC at both incubation times (Fig. 2C). MDA-MB-231 cells were the most sensitive to free-IR780. No significant loss of MCF-7 cell viability was observed even after 48 h incubation time when treated with free-IR780. In MCF-10A cells free-IR780 showed cytotoxicity at the highest concentrations after 48 h of incubation (> 1.6 μg/mL).

Concerning IR780 associated to NC, both formulations, IR-PLA NC and IR780 NC, showed similar profiles of dose-dependent cytotoxicity in MDA-MB-231 cells (24 and 48 h). The same happened for MCF-7 cells, however, at the highest concentrations, the encapsulated dye was more cytotoxic. Significant differences were observed between IR780 NC and IR-PLA NC only at the highest concentrations ($p < 0.05$). Unexpectedly, after 24 h of incubation, IR780 NC was the most cytotoxic formulation for normal MCF-10A cells. Interestingly, IR-PLA NC was less cytotoxic than IR780 NC to normal cells, which is an important aspect of selectivity. When IR780 is physically entrapped in the NC there is a significant increase ($p < 0.05$) in toxicity to cells with respect to the free dye. IR780 NC and IR-PLA NC were more cytotoxic than blank-NC and free-IR780 at all concentrations evaluated, except above 1.6 μg/mL of IR780 for MDA-MB-231 cells, where free-IR780 was more cytotoxic.

The cytotoxic concentrations for 50% of cells (CC_{50}), calculated from graph analyses, are presented in Table 2. In MCF-7 cells, the IR780 NC presented a lower CC_{50} than IR-PLA NC. There were significant differences in cell viability when MCF-7 cells were exposed to NC containing encapsulated or polymer-bound IR780 with respect to free-IR780.

The best selectivity index, calculated as the ratio of CC_{50} of normal MCF-10A vs tumor MDA-MB-231 cells, was found for IR-PLA NC with a value of 2.3. The free-IR780 and IR780 NC formulations showed no selectivity towards tumor cells (SI < 1.5) *in vitro* under our experimental conditions, in the dark (without illumination with a laser).

IR780-NC and IR-PLA NC presented significant differences in the cell viability ($P < 0.05$) with blank-NC for both tumorigenic MCF-7 and MDA-MB-231 cell lines studied (Fig. 3). No significant differences between IR780 containing formulations were observed for MDA-MB-231. At 0.8 μg/mL there were no statistically significant differences between IR780 NC and IR-PLA NC. In the absence of laser activation, IR-PLA NC was less toxic to non-tumorigenic cells than IR780-NC (Fig. 3). In contrast, IR780 NC was more toxic to the normal cell line than to both tumor cell lines (Fig. 3). This is an important aspect to increase the selectivity to tumor cells.

3.3. Photodynamic toxicity of IR780 nanocapsules in vitro and ROS quantification

To evaluate the photodynamic cytotoxicity, that is the ability of the photosensitizer to kill cells upon laser illumination, concentrations of IR780 and of polymer with low cytotoxicity in the dark were chosen. Taking into account the concentration-dependent cytotoxicity of the IR780-containing and blank NC formulations presented in the first part of this study, we selected two concentrations of IR780, namely 0.8 and 1.6 μg/mL, which correspond to polymer concentrations of 210 and 420 μg/mL, respectively. We confirm the photodynamic activity of this fluorescent dye after illumination at 808 nm producing cell death even after chemical conjugation with PLA (Fig. 4). The two human breast

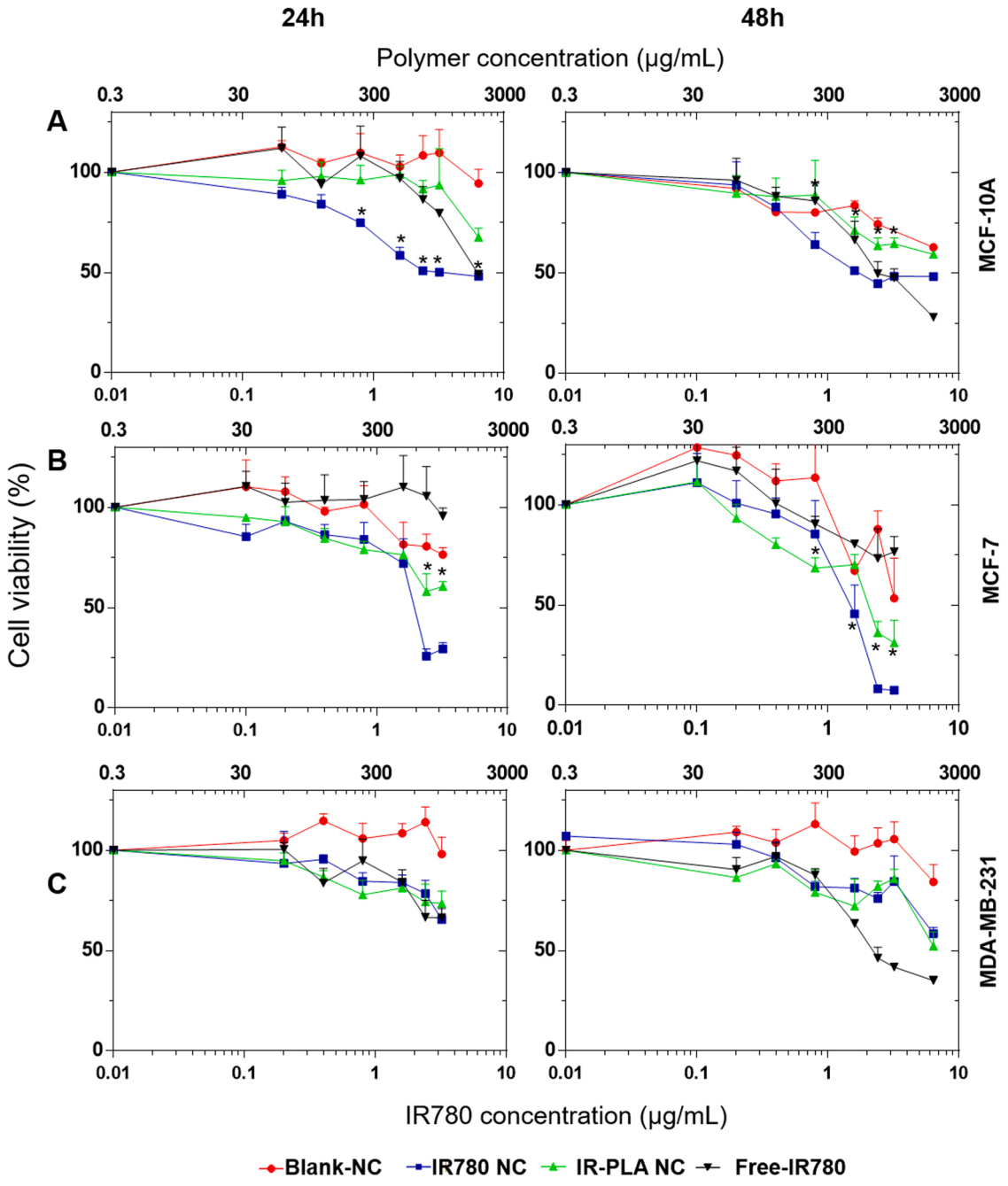

Fig. 2. Cell viability of MCF10A (A), MCF-7 (B) and MDA-MB-231 (C) cells exposed to different concentrations of nanocapsules (NC) containing IR780 (IR780 NC and IR-PLA NC) and controls (free IR780 and Blank-NC) incubated for 24 h and 48 h, in the dark. The data are the average of two independent experiments performed in triplicate (n = 6) and SD. Statistical differences were determined by comparing data by two-way ANOVA. *indicate $p < 0.05$ when comparing IR-PLA NC and IR780 NC.

Table 2
IR780 cytotoxic concentrations (CC_{50}) in different formulations toward human breast cancer cell lines (μM) in the dark at two incubation times.

Formulation	MCF-7 CC_{50} (μM)		MDA-MB-231 CC_{50} (μM)	
	24 h	48 h	24 h	48 h
Free-IR780	> 4.8 (3.2 μg/mL)	> 4.8 (3.2 μg/mL)	> 4.8 (3.2 μg/mL)	3.9 (2.64 μg/mL)
IR780 NC	2.9 (1.9 μg/mL)	2.1 (1.4 μg/mL)	> 4.8 (3.2 μg/mL)	> 4.8 (3.2 μg/mL)
IR-PLA NC	> 4.8 (3.2 μg/mL)	4.5 (3.0 μg/mL)	> 4.8 (3.2 μg/mL)	> 4.8 (3.2 μg/mL)

cancer cell lines showed different levels of susceptibility to PDT ($p < 0.05$). In the absence of laser illumination no significant loss of viability is observed for all concentrations and in all cell lines (Fig. 4A).

A decrease in MCF-7 cell viability is clearly shown for IR780 NC, IR-PLA NC and free-IR780 upon laser illumination, with statistically significant differences compared to control and blank-NC ($p < 0.05$). There were no significant differences between both NC formulations and free-IR780 at the lowest concentration ($p > 0.05$). At 1.6 μg/mL, IR780 NC decreased the cell viability more than IR-PLA NC after laser illumination ($p < 0.05$), with a decrease in cell viability values of 50% and 35%, respectively. MDA-MB-231 cells were more resistant to treatment at the lowest concentration evaluated, in agreement with the cell viability

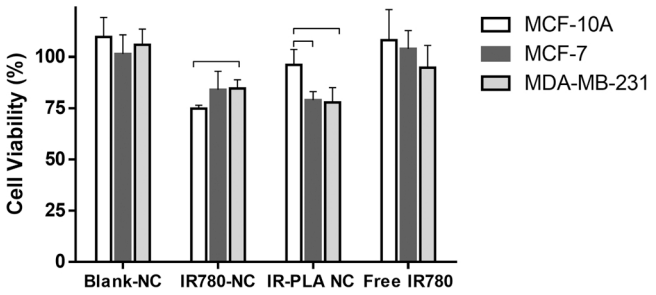

Fig. 3. Viability of MCF-7, MDA-MB-231 and MCF-10A cell lines exposed to free-IR780, IR780 NC, IR-PLA NC or blank-NC (0.8 μg/mL of IR780) for 24 h in the dark. Results are expressed as the mean ± standard deviation (n = 6). Unpaired student's *t*-test was used and $p < 0.05$ are represented by bars.

study, where no significant differences were observed in treatments with or without illumination (Fig. 4B). For this cell line, free IR780 was more cytotoxic than both NC formulations. At 1.6 μg/mL, after laser incidence, there was a greater reduction in cell viability for IR780 NC than for IR-PLA NC ($p < 0.05$). In Fig. 4C and D, we increased the doses and viability was determined 24 and 48 h after laser illumination. Thought the differences of viability are small it is evident that viability is influenced by IR780 doses (0.8; 1.6; 6.4 μg/mL of IR780) with all the formulations with similar activity after 24 h of laser illumination. However, more importantly, we observe that the time after laser exposure plays an important role in cell death, particularly in the case of IR-PLA, 24 and 48 h after laser exposure in MCF-7 cells ($p < 0.05$). IR-PLA NC presented a better photodynamic activity after 48 h of the laser illumination. This time-dependent cell death after laser exposure is not observed for free IR780 and IR780 NC.

In order to investigate the mechanism of cell death upon laser illumination, ROS generation was quantified by flow cytometry using DCFH-DA, which acts as a fluorescent probe for ROS in cells. Significant differences were observed in the ROS generation for both cells for IR780 NC, IR-PLA NC and free-IR780 upon laser illumination compared to treatment without illumination, as shown in Fig. 5.

The ability of IR780 to produce ROS under laser illumination was increased upon encapsulation in NC. The production of intracellular ROS in MCF-7 cells increased 15-fold with IR780 NC and 6-fold with IR-PLA NC compared to control (Fig. 5A). The generation of ROS under illumination happened to a larger extent in MDA-MB-231 cells (Fig. 5B), where IR780 NC increased the production of intracellular ROS 20-fold and IR-PLA NC 10-fold, both more than free-IR780. This PS, even in its free form, shows higher ability in MCF-7 cells ($p < 0.05$) to induce ROS compared to positive control with oxygen peroxide (H_2O_2) and similar ability in MDA-MB-231 cells ($p > 0.05$).

These results are in agreement with the photodynamic toxicity, where IR780 NC induced more cell death than IR-PLA NC and free IR780 under laser illumination. However, it is important to emphasize that even after the conjugation of IR780 to the polymer it did not lose its characteristics to act as a photosensitizer leading to the production of ROS upon laser illumination.

3.4. Cell apoptosis

Annexin V-FITC and propidium iodide (PI) double cell staining was used to analyze the main mechanisms of cell death via flow cytometry (Fig. 6).

All treatments (IR-PLA NC, IR780 NC and free-IR 780) reduced the percentage of live cells with significant differences with respect to control cells and to blank-NC ($p < 0.05$). There were no differences between any of the treatments regarding early apoptosis. IR780 NC and free-IR780 caused more death by necrosis than IR-PLA NC (45.4%, 42.7% and 30.6%, respectively) in MCF-7 cells (Fig. 6A). Thus, cell death by necrosis was reduced by conjugation of IR780 to PLA. MCF-7 cells were more sensitive to apoptosis induced by this photosensitizer than MDA-MB-231 cells. IR-PLA NC induced 3-fold more apoptosis than necrosis for the MDA-MB-231 cells.

In MDA-MB-231 cells the percentages of total apoptosis were 24.4% for IR-PLA NC, 18.4% for IR780 NC and 27.7% for free-IR780 (Fig. 6B). There was a proportional increase in the apoptosis rate for both NC formulations among dead cells ($p < 0.05$). Particularly, IR-PLA NC increased the percentage of death by apoptosis in MDA-MB-231. Therefore, IR780 encapsulated in NC or linked to the polymer can efficiently activate apoptotic pathways in MDA-MB-231 cells when compared with free-IR780. Free dye mainly induces cell death by necrosis.

3.5. Clonogenicity

The colony formation, or clonogenic assay, assesses cell survival *in vitro* based on the ability of a single cell to transform into a colony (at least 50 cells) and undergo uncontrolled division. Thus, it can be used to estimate the capacity of cytotoxic agents to alter tumor mitotic processes [26]. Fig. 7 shows the results of colony formation analysis, expressed as a percentage relative to control cells. Free-IR780 showed no capacity to inhibit the formation of colonies in both cancer cell lines at the concentration evaluated. In contrast, upon association to NC, whether conjugated or encapsulated, IR780 significantly inhibited the formation of clones. IR-PLA NC showed the highest anti-clonogenicity activity compared to the other formulations. Blank-NC also slightly inhibited colony formation. It is likely that the NC impaired mitotic processes in this longer incubation assay at this tested concentration, which was not detected in shorter incubation times in the viability test.

IR-PLA NC was able to inhibit colony formation to a greater extent (approximately 55%) compared with all controls for both MCF-7 and MDA-MB-231 ($p < 0.05$). There is probably an additive effect of the polymeric NC together with IR780 to reduce cell division, and probably some physical effect upon mitosis. Furthermore, for both cells significant differences in the inhibition of colony formation between free-IR780 and IR-PLA NC were observed. Thus, using IR780 conjugated to PLA polymer (IR-PLA), it was possible to reduce the formation of colonies of both breast tumor cells, which is an outstanding tool to reduce tumor growth. In the MDA-MB-231 cell line, no differences in colony formation were observed between IR780 NC and IR-PLA NC, with a reduction of clonogenicity of more than 50%. IR780 association to the NC inhibited significantly the formation of clones compared to free-IR780 ($p < 0.01$) and blank-NC ($p < 0.05$) in MDA-MB-231 cells. This quantitative result is in agreement with visual analysis of the colonies obtained from photodocumenters as shown in Fig. 7 (right).

3.6. Effects on cell migration

The effect of IR780 on the inhibition of cell migration was studied using the scratch wound assay, and significant differences were observed ($p < 0.05$) between treatments (IR-PLA NC, IR780 NC and free-IR780) and controls (Fig. 8). In this technique, a scratched area is created in a monolayer of confluent cells, and the rate of slot closure and cell migration is quantified by photographing with an inverted microscope at various time intervals [33]. We observed that the cells continued to grow when exposed to blank-NC, covering almost every scratched area for both cells by phase-contrast microscopy images analysis (Fig. 8A and B). Thus, blank-NC did not inhibit cell migration for both cell lines. In contrast, free-IR780 inhibited the migration of MCF-7 cells to a high extent than IR-PLA NC and IR780 NC ($p < 0.05$) for MCF-7 cells (Fig. 8C). IR-PLA NC and IR780 NC inhibited the cell migration more than free-IR780 in MDA-MB-231 cells (Fig. 8D). MDA-MB-231 cells were slightly less sensitive to IR780 formulations compared to MCF-7 cells. Inhibition of cell migration by IR-PLA NC occurred of almost 40% for MCF-7 and 30% for MDA-MB-231 cells.

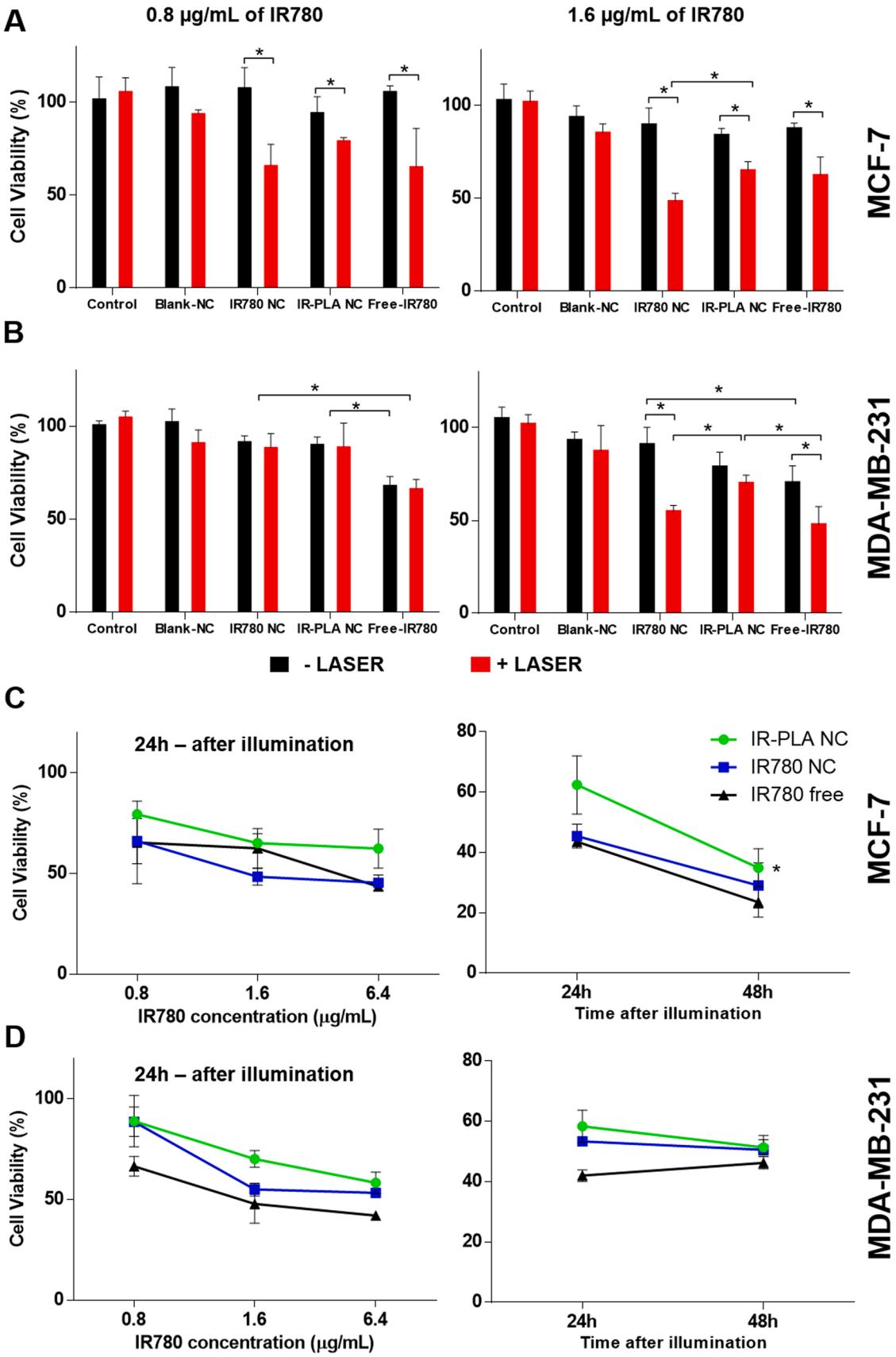

Fig. 4. MCF-7 (A) and MDA-MB-231 (B) viability when exposed to two concentrations of Blank-NC, IR780 NC or IR-PLA NC at 0.8 and 1.6 µg/mL of IR780 for 24 h, irradiated or not with 808 nm laser (1 W/cm^2) for 5 min. In (C) MCF-7 and (D) MDA-MB-231, three concentrations were used and viability determined after 24 h of laser illumination as well as after 24 and 48 h of illumination. The data are the mean values of experiments conducted in triplicate and SD. Statistical differences were determined by comparing data by two-way ANOVA. *indicate $p < 0.05$.

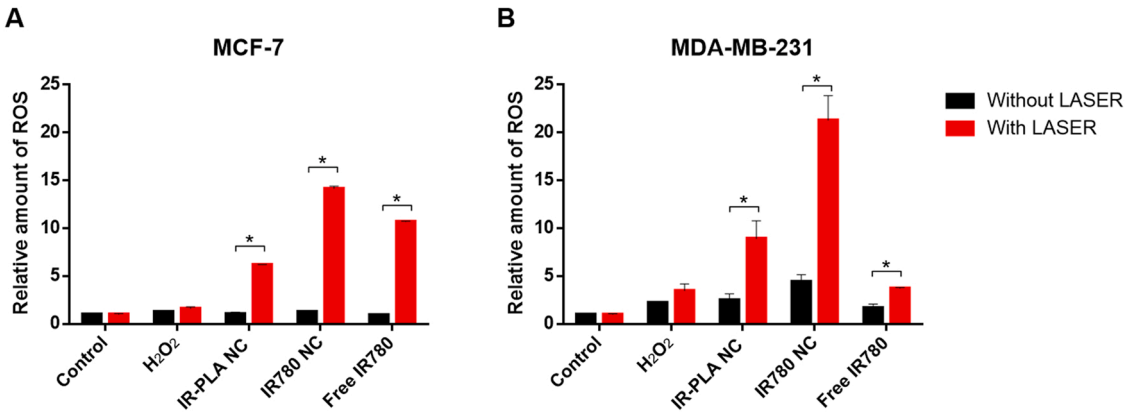

Fig. 5. ROS generation in MCF-7 (A) and MDA-MB-231 (B) cell lines when exposed to IR780 NC, IR-PLA NC or free IR780 at 1.6 μg/mL under illumination with a 808 nm laser (1 W/cm^2) for 5 min and in the dark. The basal generation of ROS by cells was normalized as 1.The data are the mean values of experiments conducted in triplicate and SD. Statistical differences were determined by comparing data by one-way ANOVA. *indicate $p < 0.05$.

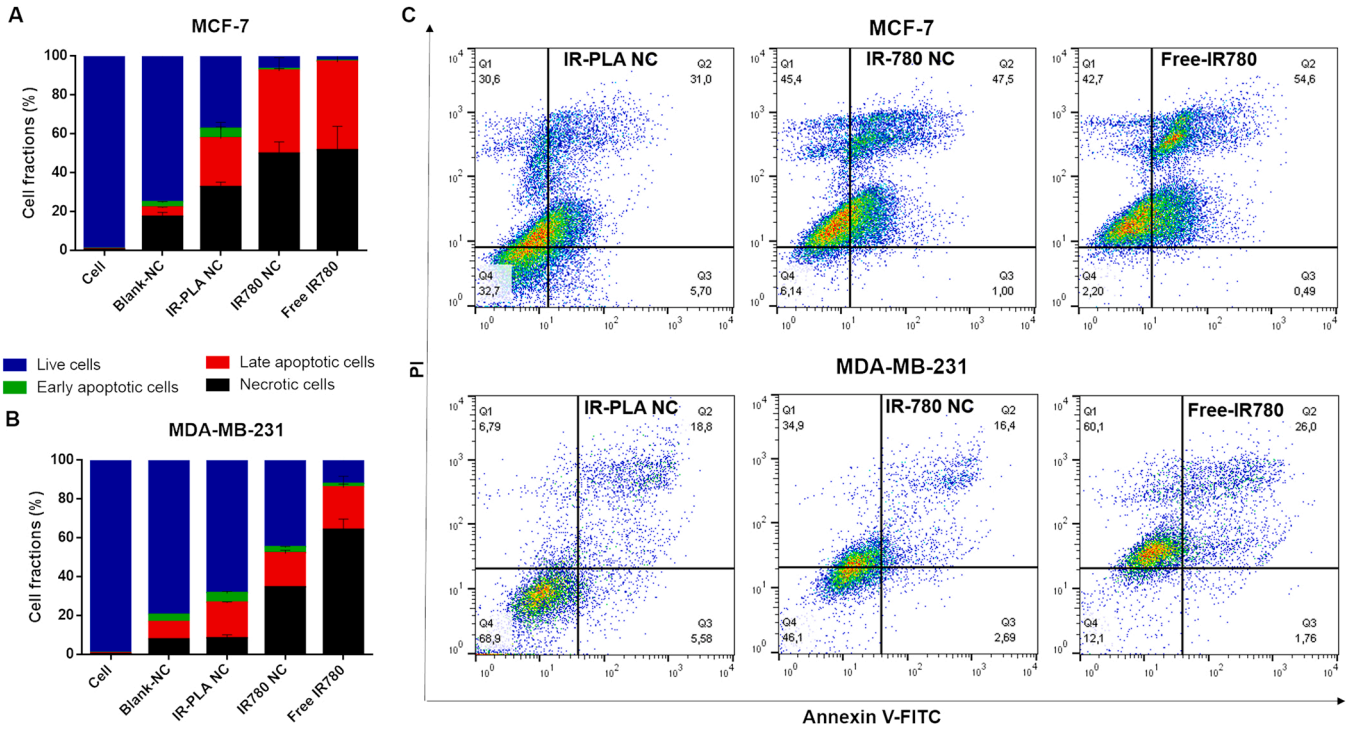

Fig. 6. Necrotic, late and early apoptotic cells and live cells after treatment with nanoparticles with 808 nm laser irradiation and followed by Annexin V-FITC and PI double staining, analyzed via flow cytometry, for MCF-7 (A) and MDA-MB-231 (B) cell lines. One representative experiment with cell percentages plotted in each quarter (C). The data are the mean values of independent experiments conducted in duplicate and SD. Statistical differences were calculated by comparing data using two-way ANOVA with Tukey's multiple comparison test. *indicate $p < 0.05$.

3.7. Cellular uptake of IR780 nanocapsules by confocal microscopy

The qualitative images of cell uptake of IR780 associated to NC was first assessed by confocal microscopy (Figs. 9 and 10). IR-PLA NC exhibited much higher fluorescence intensity in the human breast cancer cells than IR780 NC and free-IR780. Both breast tumor cells were weakly emissive after incubation with free IR780 as also observed previously with Hela cells [34]. In MCF-7 cells, IR-PLA NC were homogenously distributed inside the cytoplasm of cells suggesting high uptake of the nanoparticles (Fig. 9). Similar results of uptake were observed with MDA-MB-231 cells (Fig. 10), though the fluorescence intensity was significantly lower compared to MCF-7 cells.

MDA-MB-231 cells were less responsive to IR780 than MCF-7 cells. In the MDA-MB-231 cells almost no uptake was observed for free IR780 and IR780 NC. In the case of IR-PLA NC a more punctuate pattern of distribution of fluorescence inside the cells was identified and very low fluorescence associated to the cell membrane. Considering 2 h incubation with these NC, the images suggest a fast mechanism of NC internalization and subtle differences from the pattern observed in MCF-7 cells. These differences may be attributed to different internalization pathways between the two breast cancer cells.

3.8. Quantitative uptake of IR780 nanocapsules by flow cytometry

The qualitative results obtained by confocal microscopy were confirmed by quantitative analysis using flow cytometry (Fig. 11).

Cell association of IR780 NC and free-IR780 to both cell lines occurs in a much smaller proportion than IR-PLA NC ($p < 0.05$). Cell

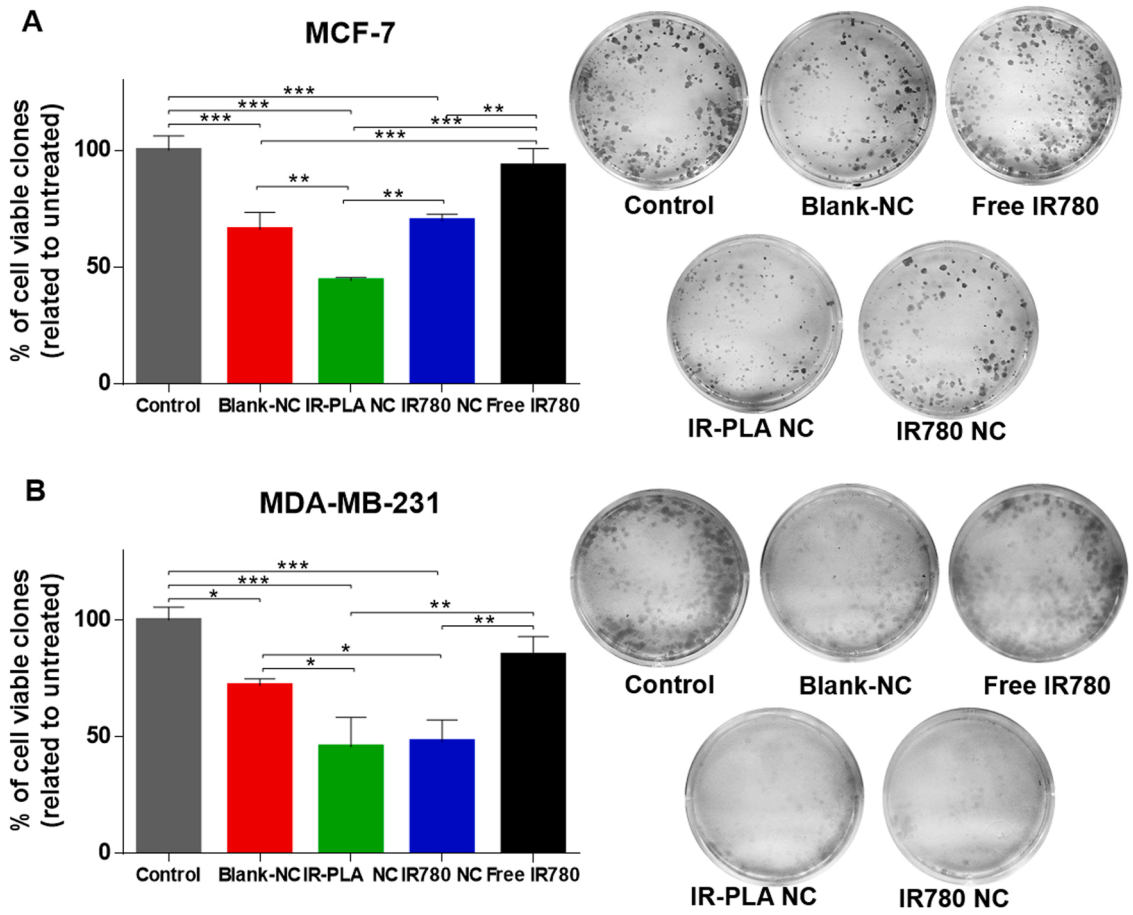

Fig. 7. Analysis of the number of colonies formed by MCF-7 (A) and MDA-MB-231 (B) cells after treatment with nanocapsules containing IR780 at 0.8 μg/mL for 24 h and observation after 2 weeks, data expressed in percentage relative to control cells. Results are expressed as the mean ± standard deviation of the triplicate. *$p < 0.05$; **$p < 0.01$ or ***$p < 0.001$; ANOVA followed by Bonferroni.

association of IR780 NC and free-IR780 is clearly dose-dependent, whereas a saturation profile of cell-associated fluorescence was observed with IR-PLA NC. In MCF-7 cells, in which the association of NC was higher, dose-dependent interaction with cells is clearly observed until saturation is reached. We observe a linear increase in fluorescence associated to cells with an increase in free-dye concentration (Fig. 11A and B). IR780 NC showed intermediate behavior between free dye and internalization of IR-PLA NC, probably because a fraction of the dye is released from the NC and a part is attached to the nanocarrier. For IR-PLA NC the uptake occurs in a time-dependent manner in MCF-7 cells (Fig. 11C), while there was no difference for IR780 NC or free IR780 uptake along time. In MDA-MB-231 cells (Fig. 11D), the uptake increased in the first 2 h when it reaches a plateau.

4. Discussion

Encapsulation efficiencies close to 100% were obtained for IR780 loading in our NC. This demonstrates that our system is a good carrier for this compound and it is expected because IR780 presents high lipophilicity and affinity for the oily nucleus of the NC, as demonstrated previously [23]. The mean hydrodynamic diameter of NC around 120 nm is an important parameter in cancer treatments administered by the intravenous route. Both polymeric NC, despite the mode of IR780 association to the carrier showed similar mean hydrodynamic diameters with homogeneously distributed sizes in agreement with morphological analysis using atomic force microscopy (AFM) of blank-NC, IR780 NC and IR-PLA NC previously reported by our group [23]. It is well accepted that particles with a mean size in the range of 20–200 nm administered intravenously are able to permeate through the fenestrations of tumor abnormal vessels formed during tumor angiogenesis, but they cannot enter the narrow endothelial fenestrations of normal tissues [35]. This mechanism, called the enhanced permeability and retention effect (EPR effect), favors accumulation of the nanoparticles in the tumor sites compared to normal tissues.

Although several studies in the literature report the effect of nanoparticles containing encapsulated IR780 on cell viability, as summarized in the extensive review by ALVES et al. [12], the polymer-IR780 conjugate IR-PLA proposed in this study is a new and original chemical entity. We synthesized this conjugate to ensure stable association to the NC and consequently alter the cell association profile and biodistribution of IR780 as it remains within the NC, and therefore allow reliable tracking of the NC during *in vitro* cell imaging and *in vivo* biodistribution studies. Stable labeling of the NC was demonstrated in our previous release studies, with noticeable differences between covalently bound IR-PLA and physically encapsulated IR780 [23]. In the present study, comparative cell viability between IR780 and IR-PLA gives insights into the effect of the chemical modification of IR780 on its antitumor activity and on the selectivity between normal and tumorigenic cell lines, as well as into the main mechanism of cell death. Our confocal microscopy images demonstrate that covalent attachment of IR780 to PLA modifies the pathway of IR780 internalization by cells, whereby IR-PLA and the fraction of IR780 that remains within the NC are more likely to reach within the cells.

IR-PLA exhibited the highest selectivity index and low toxicity without laser illumination although we did not observe high selectivity against tumor cells for any of the three formulations. We evidenced that

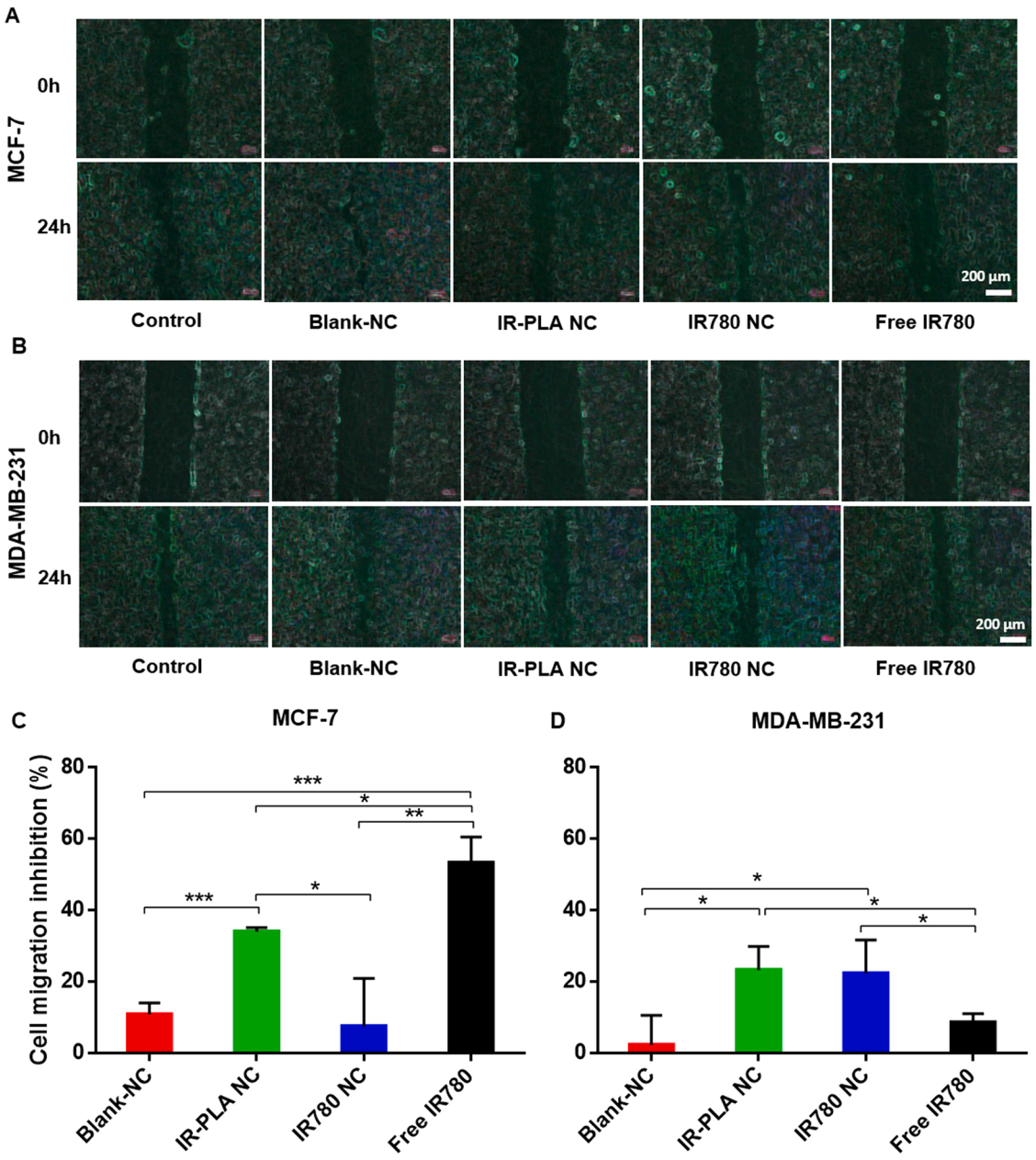

Fig. 8. Cell migration inhibition. Phase-contrast microscopy images of wells for MCF-7 (A) and MDA-MB-231 (B) cells incubated with blank-NC, IR-PLA NC, IR780 NC and free IR780 (1.6 µg/mL of IR780) and bar graphs (C,D) with the percentage of cell migration inhibition. The results are means ± SD of two independent experiments conducted in replicate. Statistical differences were determined by one-way ANOVA. *$p < 0.05$, **$p < 0.01$ or ***$p < 0.001$. Bars in images corresponds to 200 µm.

in the absence of laser illumination the IR780 associated NC were more toxic to both tumor cell lines than to the normal cell line. Most published studies did not report high cytotoxic activity for free or encapsulated IR780 without laser irradiation [12]. An ideal photosensitizer should not be toxic to cells without photo-activation, but preferential accumulation in tumor cells is desirable. Our study demonstrates low toxicity of IR780 below 3 µg/mL for MCF-7 cells, without laser illumination. In agreement with previous cell viability studies with other nanocarriers containing IR780, Yue and collegues [32] studied the cytotoxicity of heparin and folic acid nanoparticles in MCF-7 cells where free-IR780 without laser illumination did not show cytotoxicity to the cells after 12 h of treatment at a concentration of 3 µg/mL. Chen and collegues [36] developed micelles containing encapsulated IR780 and evaluated their cytotoxicity in pancreatic tumor cells, for which free-IR780 without laser illumination was not able to decrease the cell viability by more than 20%. Thus, the cytotoxicity seems to be cell type and time dependent. Furthermore, its activity was only clearly seen after laser activation at 808 nm. The majority of the studies report that illumination with a laser is essential to reduce the viability of numerous tumor cell lines with IR780 free or associated to nanocarriers [12]. Therefore, in the next step we evaluate the toxicity of IR780 or IR-PLA associated to NC after illumination with a 808 nm laser.

In many studies in the literature, free-IR780 showed a significant drop in cell viability after laser irradiation. We observed that IR780 conjugated to PLA maintains its photodynamic activity, but it is likely that conjugation can modify the pathway of IR780 internalization by cells and the rate of IR780 release in the cell organelles. Lin and colleagues [37] conjugated IR780 to hyaluronic acid and the nanoparticles were self-assembled with a hydrophobic core and hydrophilic shell in aqueous conditions . Even after the conjugation of IR780, the

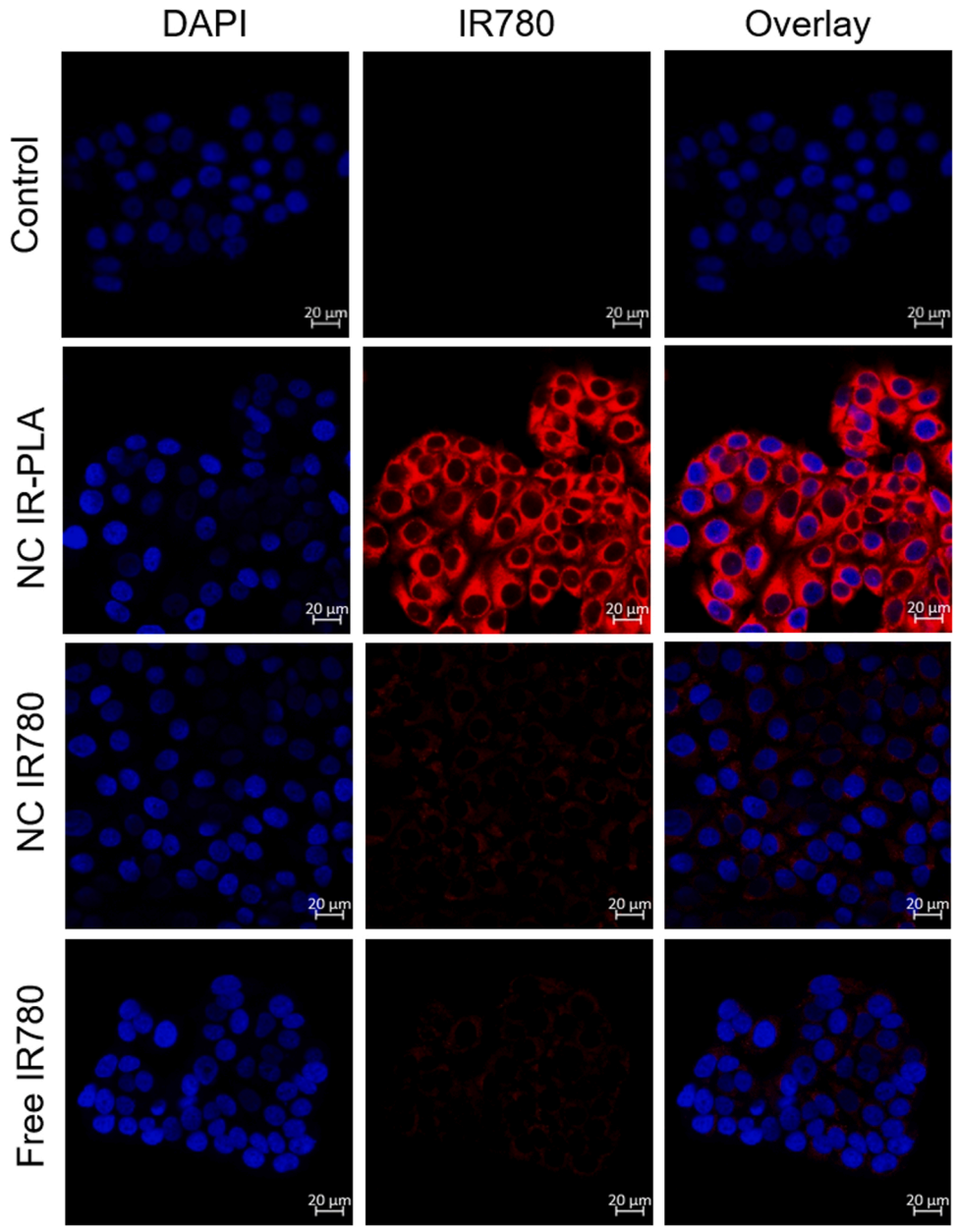

Fig. 9. Confocal laser scanning images of MCF-7 cells, incubated with IR-PLA NC, IR780 NC, free-IR780, or control cells (without any treatment) at a concentration of 1.6 μg/mL (2.4 μM) of IR780 and equivalent concentrations of polymers, incubated for 2 h in the dark. The white bars correspond to 20 μm, in 40× magnification.

nanoparticles exhibited remarkable cytotoxicity upon 808 nm laser irradiation (1 W/cm^2) for 3 min, at IR780 concentrations of 0.625 and 1.25 μg/mL. Previous works with nanocarriers containing IR780 presented remarkable cytotoxicity only at higher concentrations, in agreement with our study. Lian and col. [37] developed IR780 loaded nanoparticles based on human serum albumin and found a decrease in cell viability at 1 and 1.5 μg/mL, similar to our findings with IR780 NC at 1.6 μg/mL, i.e. viability around 75% without laser and almost 50% with laser illumination for 1.5 μg/mL of IR780 in prostate cancer cells (22RV1). Similar results were found by Li and col. with IR780-loaded PLGA nanoparticles in 4T1 mouse breast cancer cells after 24 and 48 h [15].

The differences in photodynamic activity of IR780-NC and IR-PLA NC with NIR light illumination with respect to the nanoformulations revised by Alves et al. [12] are related to the differences in concentrations used in the experiments. Three studies cited in this revision used the following concentrations of IR780: 4.18 μg/mL [38] and 12.5 μg/mL [13] for MCF-7 cells; and 20 μg/mL [39] for MDA-MB-231, for example. We used two concentration of IR780 in the phototoxicity assay (0.8 and 1.6 μg/mL) and they were chosen based on the cytotoxicity of similar blank-NC (a concentration of blank-NC, which was not toxic to the cells). Unfortunately, our concentration is limited by the amount of IR780 conjugated to the polymer. As one unit of IR780 is attached at the PLA polymer chain end, its concentration in our NC is correlated to that of polymer in the formulation, i.e. 21.6 μg of IR780 per mg of PLA polymer. In our experimental design, for comparison purposes, the NC containing IR780 encapsulated were prepared at the same concentrations. That is why we have a low amount of IR780. This is a limitation of our formulations that can be improved by freeze-drying the nanocapsules to concentrate them before administration.

Furthermore, IR780 kept its ability to produce ROS upon laser illumination even after conjugation to the polymer, although to a lower extent. IR-PLA NC in the MDA-MB 231 cell line was better than free-IR780 to induce ROS production, inhibit cell migration, and reduce

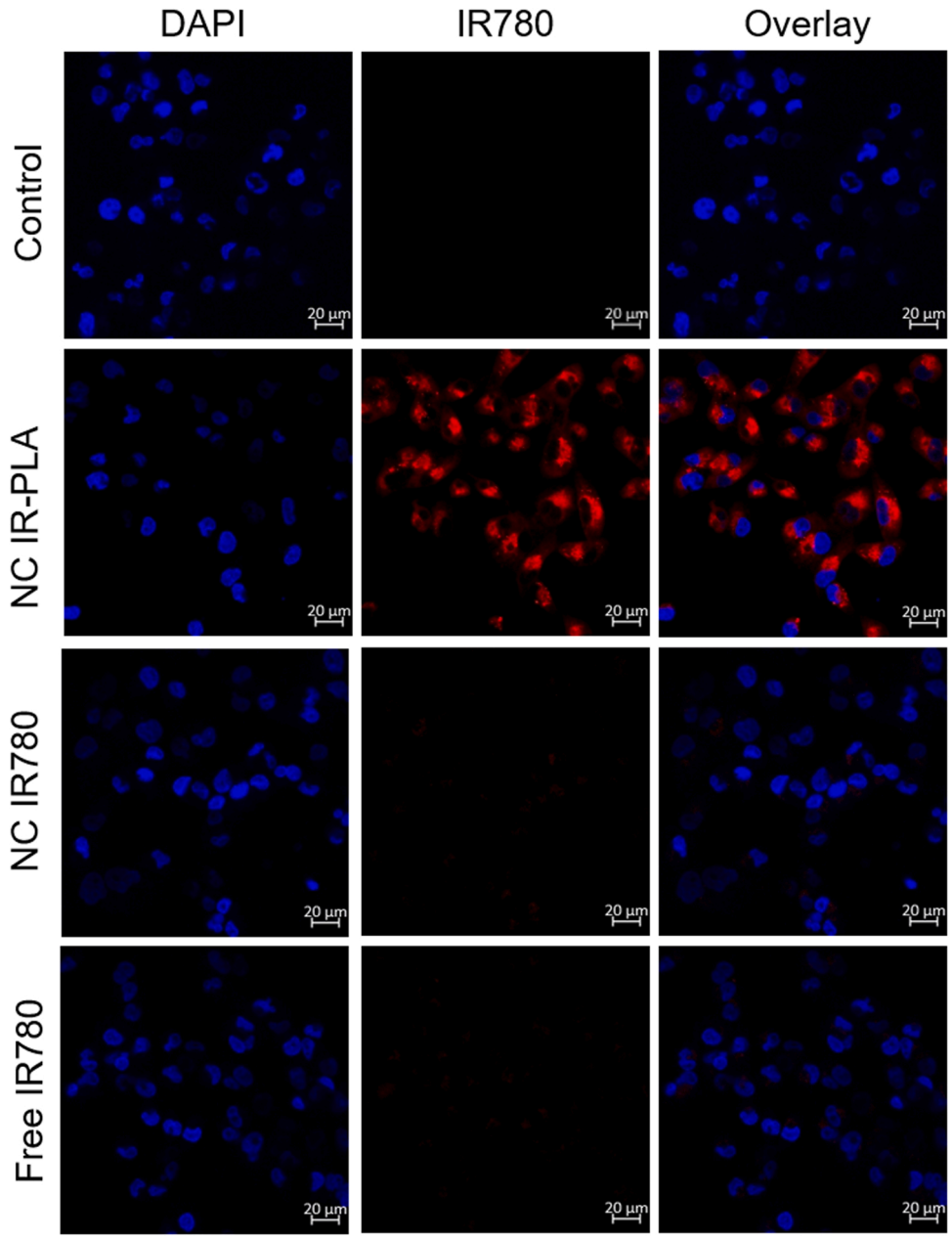

Fig. 10. Confocal laser scanning images of MDA-MB-231 cells, incubated with IR-PLA NC, IR780 NC, free-IR780, or control cells (without any treatment) at a concentration of 1.6 μg/mL (2.4 μM) of IR780 and equivalent concentrations of polymers, incubated for 2 h in the dark. The white bars correspond to 20 μm, in 40× magnification.

clonogenicity. In contrast, MCF-7 cells were more responsive to free-IR780. Furthermore, it was possible to track NC in the cells with IR-PLA in a good extent *in vitro*, as demonstrated here in the uptake studies by confocal microscopy and flow cytometry. This was also demonstrated *in vivo*, in a previous report by our group [21]. IR-PLA NC efficiently activated apoptotic pathways in MDA-MB-231, the triple negative breast tumor cell line. IR-PLA NC also reduced colony formation (55%) and cell migration by 40% for MCF-7 and 30% for MDA-MB-231.

IR780 NC and free IR780 lead to more cell death for MCF-7 and MDA-MB-231 cells than IR-PLA NC. However, in MCF-7 cells, for all treatments, half of the cells were killed by the apoptotic pathway and half by necrosis. Similar results were reported by Li and colleagues [14] with IR780 encapsulated in nanostructured lipid carriers (NLCs) after laser irradiation in 4T1-luc cells, where 22.7% of the cells died by necrosis and 28.9% were apoptotic cells.

Among the non-live MDA-MB-231 cells treated with IR-PLA NC, approximately 70% were apoptotic. MDA-MB-231 is an invasive breast cancer cell line, negative for estrogen, progesterone and HER2 receptors. It is more aggressive and related to poor prognosis since it less sensitive to conventional treatment. These results are important because apoptosis pathway of death is a vital programmed event that eliminates damaged cells without the involvement of inflammatory cells. In contrast, necrosis is a chaotic and non-programmed cell death pathway, in general less effective than apoptosis in patient outcome treated by PDT [40]. The mechanism of cell death induced by photosensitizers can occur via programmed (apoptotic) or non-programmed (necrotic or autophagic) pathways, depending on the localization of the photosensitizer in the cell [4]. Generally, when it is distributed to the nucleus, Golgi complex, and mitochondria, the mainly death pathway occurs by apoptosis, the type-I mode of cell death in PDT. Necrosis is common when the photosensitizer induces damages at the plasma membrane

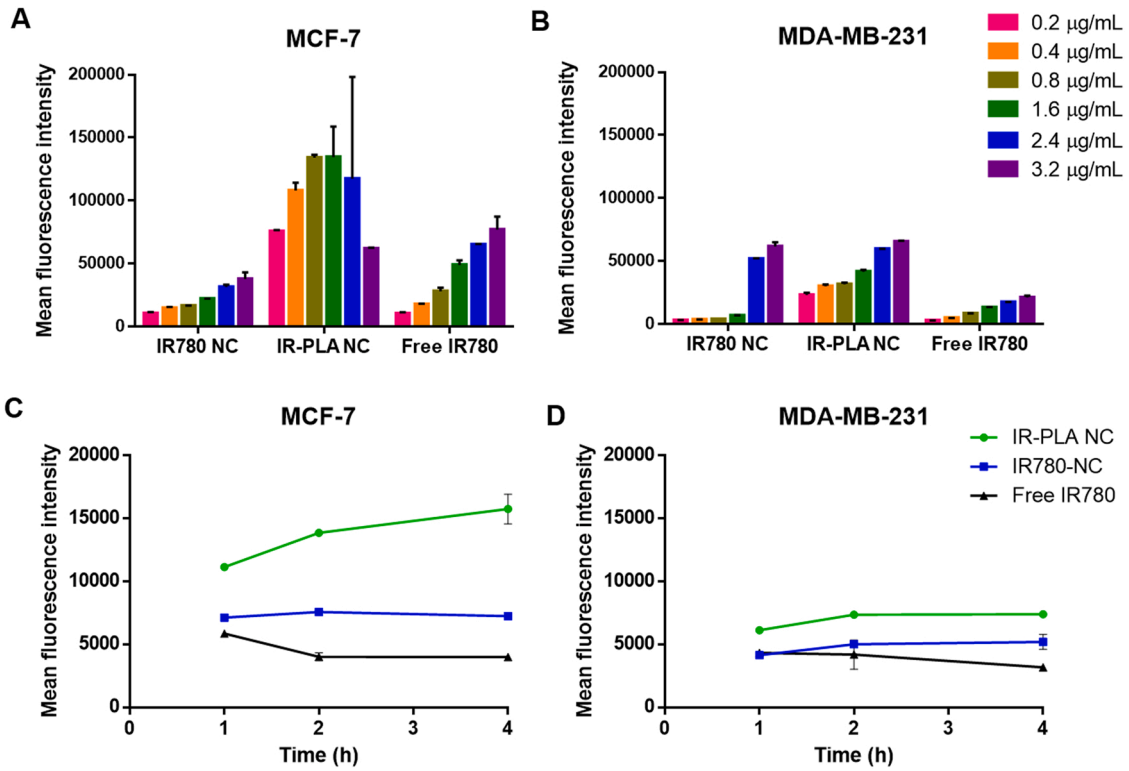

Fig. 11. Dose-dependent uptake studies normalized by mean fluorescence intensity of IR780 in breast tumor cells MCF-7 (A) and MDA-MB-231 (B) incubated with IR780 associated to nanocapsules for 2 h at different concentrations. Time-dependent uptake for MCF-7 (C) and MDA-MB-231 (D) cells after incubation for 1, 2 or 4 h, determined by flow cytometry (1.6 µg/mL). The data are the mean of two independent experiments performed in triplicate (n = 6) and SD.

[41]. Apoptosis is a preferential pathway to kill tumor cells because of the response caused by the immunological system. Both mechanism of death, apoptosis and necrosis, can attract phagocytes. In contrast, when the process is triggered by apoptosis, phagocytic cells such as macrophages secrete immune-suppressive cytokines upon engulfing apoptotic cells, unlike the necrosis process in which necrotic cells secrete proinflammatory cytokines [42].

The ability of IR780 to preferentially accumulate in tumor cell mitochondria was already demonstrated [28,6,34]. In a comparative study, the cellular uptake of IR780 was significantly higher in tumor cells than in non-tumorigenic cells, probably mediated by OATP1B, a subtype of organic anion transporter peptides (OATP). The mitochondria is an efficient target to enhance PDT outcomes, because it is related to photodamage in antiapoptotic membrane-bound proteins including B-cell lymphoma protein 2 (Bcl-2) and Bcl-xL [40]. It can lead to the permeabilization of the membrane resulting in the activation of caspases, with consequent release of cytochrome c from mitochondria and apoptosis.

Besides that, the mechanism of cell death is probably mediated by ROS production, which activates the apoptosis pathway. Upon laser illumination, IR780 NC reduced the cell viability to a higher extent than IR-PLA NC and free-IR780. However, ROS induction by IR-PLA NC was higher than free-IR780, for MDA-MB-231 cells. The cell uptake and confocal images indicated that free-IR780 and IR-PLA NC entry in cells by different pathways and are trafficked to different organelles inside cells.

It is therefore likely that covalent attachment to the polymer did not inhibit IR780 photodynamic activity but delayed it, compared to the free dye. Thus, after polymer degradation inside the cells IR780 is slowly released from IR-PLA NC and can be activated more efficiently by light. ROS production induced by photosensitizers usually has a short lifetime (less than 3.5 µs) and short diffusion distance (up to 20 nm), which may limit the therapeutic effects [43]. ROS generated in the cytoplasm may be quenched before acting on the DNA in cell nuclei [43]. Thus, intracytoplasmic IR780 with long-lasting release may induce ROS for longer times improving DNA damage in tumor cells.

The clonogenic assay is a robust assessment of the clonogenic survival and expansion of tumor cells. Interestingly, in this long incubation experiment, we observed that IR-PLA NC reduced the colony formation to a larger extent than IR780 NC and free IR780 in MCF-7 and MDA-MB-231 cells. This is in agreement with IR780 long-lasting release from conjugated polymer. This means that both cancer cell lines lost their capacity to produce a large number of progeny upon exposure to IR-PLA NC. It is an important result for the prevention of breast cancer recurrences [26]. Furthermore, IR-PLA NC demonstrated a beneficial effect on the growth of tumors inhibiting cell migration, since the lack of regulation of this process drives the progression of tumor invasion and metastasis.

Additionally, this study clearly demonstrates a huge difference between modes of association of IR780 with the two nanocapsules formulations in their interactions with cells. This behavior cannot be attributed to particle size and surface charge differences between formulations. Furthermore, free IR780 and IR780 NC exhibited similar uptake profiles. When only physically associated with NC, our data strongly indicates that IR780 is release/partitioned from the NC to serum proteins in the medium or to cell membranes. Our results evidence different uptake mechanisms for free-IR780 and IR-PLA NC. The results suggest that IR780 may be released from the NC in the cell culture medium before its cell internalization, as demonstrated in the absence of cells in a recent study [22] , where 70% transfer of IR780 from IR780 NC to serum proteins was evidenced by asymmetric flow field-flow fractionation technique (AsF4) [21,22].

In addition, it is clearly shown from linear increases in cell-associated fluorescence with increases in IR-PLA NC concentration that a saturable profile is observed in the quantitative uptake studies using flow cytometry. This behavior is generally correlated with

receptor-mediated endocytic pathways of nanoparticle internalization. In contrast, free-dye transfer to cell membrane, for example, is not expected to be a saturated process because it is based on molecular partitioning of the lipophilic dye toward cell bilayers. In fact, the transfer of the PS to cell membranes is also in agreement with high cell death by necrosis triggered by free-IR780 and IR780 NC.

The total uptake of all formulations was higher in MCF-7 than in MDA-MB-231 cells. This data is in agreement with differences observed between the two cell lines in viability studies, clonogenicity, cell death mechanism and effects on cell migration. In a recent study with the same NC [23], a high level of fluorescence associated with the macrophage-like J774-A.1 cell line was observed upon incubation with IR780 NC and free IR780, contrary to breast tumor cells (non-phagocytic cells). It is likely that the high phagocytic index of macrophages, which employ fast and multiple mechanisms of endocytosis play a role in this difference [44,45].

The MCF-7 cell line is extensively used for *in vitro* breast cancer studies, as it has characteristics of the breast epithelial tissue, such as the presence of estrogen and progesterone receptors on the cell membrane [46]. In contrast, the MDA-MB-231 cell line is negative for estrogen, progesterone and HER2 receptors, and is used as a research model for triple negative cancer type [47]. Therefore, the latter are more aggressive and related to a worse prognosis and are more resistant to treatment. MDA-MB-231 cells are significantly less responsive to IR780, despite its encapsulation in NC. It is likely that IR780 entry into the cells is facilitated by membrane receptors present in MCF-7 and absent in MDA-MB-231 cells. IR780 entry into cells may be mediated by the organic anion-transporting polypeptide (OATP) superfamily transporters expressed in various type of tumors with poor prognosis [7]. These transmembrane protein transporters play a role in the absorption, distribution and excretion of endogenous hormones and their conjugates, exogenous molecules and drugs. They are closely related to the prognosis of tumors. Some findings showed that OATP1 was barely detectable in non-malignant mammary epithelial cells [48] and it also plays a role in regulating the growth of hormone-dependent breast tumors [49]. Thus, the differences in the uptake of IR780 between the two cell lines studied herein may be related to the expression of these transporters in their cell membranes. In contrast, the fraction of photosensitizer that remains associated to the NC follows pathways of receptor mediated-endocytosis. The endocytic pathway of internalization is adopted by polymeric nanoparticles of 20–200 nm diameter-range, such as macropinocytosis and clathrin or caveolin-mediated endocytosis, which is not likely to involve such cell membrane transporters [50,51,45,52].

Altogether, our results demonstrate the applicability of sterically stabilized PEG-PLA polymeric NC containing IR-PLA in order to conduct reliable cell internalization studies and to induce breast cancer cell death upon laser illumination. The behavior of the physically encapsulated IR780 in the NC was similar to that of free IR780, indicating another pathway of interaction with cells. Surprisingly, most of the works published in the literature were carried out with IR780 physically encapsulated in different types of nanocarriers, as extensively reviewed [12].

5. Conclusion

The conjugation of IR780 to PLA polymer (IR-PLA NC) provides stability in association with cells in biological media and a profile of cell interaction indicative of receptor-mediated endocytosis, which is consistent with the internalization of nanoparticles itself. The mechanism of death involves a significant percentage of apoptosis with a significant reduction of necrosis in this case. IR-PLA NC are the less cytotoxic formulation for normal breast cells. Additionally, *in vitro* clonogenicity results reinforces the best behavior of IR-PLA NC, since it is often strongly correlated with tumorigenicity *in vivo* with characteristics of cancerous stem cells. High inhibition of migration was also observed with IR-PLA NC, indicating potential to reduce metastasis in breast tumors. Thus, our results suggest that IR-PLA NC shows promising features to produce longer release of ROS inside cells to be investigated as photosensitizer in PDT of animals and humans with breast cancer. This nanocarrier can also be used as a platform, where different types of ligands can be conjugated to polymer to target cells and microorganisms using fluorescent polymeric nanocapsules to monitor *in vivo* drug distribution and investigate antitumor activity.

Funding

This work was supported by the Minas Gerais Research Funding Foundation (FAPEMIG) grants (#APQ-02576-18, #APQ-02864-16 and NANOBIOMG-Network # 7-14); from National Council for Scientific and Technological Development (CNPq/Brazil) grants (#436460/2018-1 and #313602/2019-0, BRICS-STI# 442351/2017-8), from CAPES post-doctoral scholarship to Raoni P. Siqueira (INCT-NANOFARMA-Grant #465687/2014-8) and from PROPPi/UFOP.

CRediT authorship contribution statement

Marina Guimarães Carvalho Machado: Conceptualization, Data curation, Formal analysis, Investigation, Methodology, Writing – original draft, Writing – review & editing. **Maria Alice de Oliveira:** Investigation. **Elisa Gomes Lanna:** Investigation, Methodology. **Raoni Pais Siqueira:** Investigation, Methodology. **Gwenaelle Pound-Lana:** Conceptualization, Formal analysis, Supervision, Writing – review & editing. **Renata Tupinambá Branquinho:** Investigation, Methodology. **Vanessa Carla Furtado Mosqueira:** Conceptualization, Formal analysis, Project administration, Resources, Funding acquisition, Supervision, Writing – review & editing.

Conflict of interest statement

We have no conflict of interest to declare.

Acknowledgments

The authors thank CAPES/Brazil for doctoral scholarship to MGCM, MAO of graduated students. We acknowledge Dra. Nívia C.N. Paiva for her skillful assistance with confocal laser microscopy, as well as Flow Cytometry Facility from LMUCF/NUPEB/UFOP, which were acquired with financial support of CT-Infra FINEP/Brazil.

References

[1] Cancer. Pan American Health Organization (PAHO) [Internet]. [cited 2021 Jul 20]. Available from: https://www.paho.org/pt/topicos/cancer.
[2] Brasil. Ministério da saúde. Instituto Nacional de Câncer. Estatísticas de câncer [Internet]. 2020 [cited 2020 Nov 27]. Available from: https://www.inca.gov.br/numeros-de-cancer.
[3] D. Gao, X. Guo, X. Zhang, S. Chen, Y. Wang, T. Chen, G. Huang, Y. Gao, Z. Tian, Z. Yang, Multifunctional phototheranostic nanomedicine for cancer imaging and treatment, Materials Today Bio 5 (2020), 100035, https://doi.org/10.1016/j.mtbio.2019.100035.
[4] H.O. Alsaab, M.S. Alghamdi, A.S. Alotaibi, R. Alzhrani, F. Alwuthaynani, Y. S. Althobaiti, A.H. Almalki, S. Sau, A.K. Iyer, Progress in clinical trials of photodynamic therapy for solid tumors and the role of nanomedicine, Cancers 12 (2020) 1–26.
[5] C. von Roemeling, W. Jiang, C.K. Chan, I.L. Weissman, B.Y.S. Kim, Breaking Down the Barriers to Precision Cancer Nanomedicine. Trends Biotechnol 35 (2) (2017) 159–171, https://doi.org/10.1016/j.tibtech.2016.07.006.
[6] C. Zhang, T. Liu, Y. Su, S. Luo, Y. Zhu, X. Tan, S. Fan, L. Zhang, Y. Zhou, T. Cheng, C. Shi, A near-infrared fluorescent heptamethine indocyanine dye with preferential tumor accumulation for in vivo imaging, Biomaterials 31 (25) (2010) 6612–6617.
[7] N. THAKKAR, A.C. Lockhart, W. Lee, Role of organic anion-transporting polypeptides (OATPs) in cancer therapy, AAPS J. 17 (3) (2015) 535–545, https://doi.org/10.1208/s12248-015-9740-x.
[8] E. Zhang, S. Luo, X. Tan, C. Shi, Mechanistic study of IR-780 dye as a potential tumor targeting and drug delivery agent, Biomaterials 35 (2) (2014) 771–778.

[9] X. Yi, J. Zhang, F. Yan, Z. Lu, J. Huang, C. Pan, J. Yuan, W. Zheng, K. Zhang, D. Wei, W. He, J. Yuan, Synthesis of IR-780 dye-conjugated abiraterone for prostate cancer imaging and therapy, Int. J. Oncol. 49 (5) (2016) 1911–1920.

[10] P. Mroz, A. Yaroslavsky, G.B. Kharkwal, M.R. Hamblin, Cell Death pathways in photodynamic therapy of cancer, Cancers 3 (2011) 2516–2539.

[11] A.P. Castano, T.N. Demidova, M.R. Hamblin, Mechanisms in photodynamic therapy: part one - photosensitizers, photochemistry and cellular localization, Photo Photodyn. Ther. 1 (2004) 279–293.

[12] C.G. Alves, R. Lima-Sousa, D. de Melo-Diogo, R.O. Louro, I.J. Correia, IR780 based nanomaterials for cancer imaging and photothermal, photodynamic and combinatorial therapies, Int. J. Pharm. 542 (1–2) (2018) 164–175.

[13] C. Jiang, H. Cheng, A. Yuan, X. Tang, J. Wu, Y. Hu, Hydrophobic IR780 encapsulated in biodegradable human serum albumin nanoparticles for photothermal and photodynamic therapy, Acta Biomater. 14 (2015) 61–69.

[14] H. Li, K. Wang, X. Yang, Y. Zhou, Q. Ping, D. Oupicky, M. Sun, Dual-function nanostructured lipid carriers to deliver IR780 for breast cancer treatment: anti-metastatic and photothermal anti-tumor therapy, Acta Biomater. 53 (2017) 399–413.

[15] J. Li, H. Hu, Z. Jiang, S. Chen, Y. Pan, Q. Guo, Q. Xing, Z. Jing, Y. Li, L. Wang, Near-infrared-induced IR780-loaded PLGA nanoparticles for photothermal therapy to treat breast cancer metastasis in bones, RCS Adv. 9 (2019) 35976–35983, https://doi.org/10.1039/C9RA05813C.

[16] C. Pais-Silva, D.D.E. Melo-Diogo, I.J. Correia, IR780-loaded TPGS-TOS micelles for breast cancer photodynamic therapy, Eur. J. Pharm. Biopharm. 113 (2017) 108–117.

[17] K. Wang, Y. Zhang, J. Wang, A. Yuan, M. Sun, J. Wu, Y. Hu, Self-assembled IR780-loaded transferrin nanoparticles as an imaging, targeting and PDT/PTT agent for cancer therapy, Sci. Rep. 6 (1) (2016) 27421–27432.

[18] A. Yuan, X. Qiu, X. Tang, W. Liu, J. Wu, Y. Hu, Self-assembled PEG-IR-780-C13 micelle as a targeting, safe and highly-effective photothermal agent for in vivo imaging and cancer therapy, Biomaterials 51 (2015) 184–193, https://doi.org/10.1016/j.biomaterials.2015.01.069.

[19] M. Ghezzi, S. Pescina, C. Padula, P. Santi, E. Del Favero, L. Cantù, S. Nicoli, Polymeric micelles in drug delivery: an insight of the techniques for their characterization and assessment in biorelevant conditions, J. Control. Release 332 (2021) 312–336.

[20] H. Polat, G. Kutluay, M. Polat, Analysis of dilution induced disintegration of micellar drug carriers in the presence of inter and intra micellar species, Colloids Surf. A 601 (2020), 124989.

[21] M.A. De Oliveira, M. Guimarães Carvalho Machado, S.E. Dias Silva, T. Leite Nascimento, E. Martins Lima, G. Pound-Lana, V.C.F. Mosqueira, IR780-polymer conjugates for stable near-infrared labeling of biodegradable polyester-based nanocarriers, Eur. Polym. J. 120 (2019), 109255, https://doi.org/10.1016/j.eurpolymj.2019.109255 (June).

[22] M.A. de Oliveira, G. Pound-Lana, P. Capelari-Oliveira, T.G. Pontífice, S.E.D. Silva, M.G.C. Machado, B.B. Postacchini, V.C.F. Mosqueira, Release, transfer and partition of fluorescent dyes from polymeric nanocarriers to serum proteins monitored by asymmetric flow field-flow fractionation, J Chromatogr A. 1641 (2021), 461959, https://doi.org/10.1016/j.chroma.2021.461959.

[23] M.G.C. Machado, G. Pound-Lana, M.A. de Oliveira, E.G. Lanna, M.C.P. Fialho, A. de Brito, A.P. Barboza, R.D. Aguiar-Soares, V.C.F. Mosqueira, Labeling PLA-PEG nanocarriers with IR780: physical entrapment versus covalent attachment to polylactide, Drug Deliv. Transl. Res. 10 (6) (2020) 1626–1643, https://doi.org/10.1007/s13346-020-00812-6.

[24] G. Pound-Lana, J.M. Rabanel, P. Hildgen, V.C.F. Mosqueira, Functional polylactide via ring-opening copolymerisation with allyl, benzyl and propargyl glycidyl ethers, Eur. Polym. J. 90 (2017) 344–353.

[25] T. Mosmann, Rapid colorimetric assay for cellular growth and survival: application to proliferation and cytotoxicity assays, J. Immunol. Methods 65 (1–2) (1983) 55–63.

[26] N.A. Franken, H.M. Rodermond, J. Stap, J. Haveman, C. van Bree, Clonogenic assay of cells in vitro, Nat. Protoc. 1 (5) (2006) 2315–2319.

[27] H.A. Hirsch, D. Iliopoulos, P.N. Tsichlis, K. Struhl, Metformin selectively targets cancer stem cells, and acts together with chemotherapy to block tumor growth and prolong remission, Cancer Res. 19 (2009) 7507–7512.

[28] Y. Wang, T. Liu, E. Zhang, S. Luo, X. Tan, C. Shi, Preferential accumulation of the near infrared heptamethine dye IR-780 in the mitochondria of drug-resistant lung cancer cells, Biomaterials 35 (13) (2014) 4116–4124, https://doi.org/10.1016/j.biomaterials.2014.01.061.

[29] S. Li, J. Johnson, A. Peck, Q. Xie, Near infrared fluorescent imaging of brain tumor with IR780 dye incorporated phospholipid nanoparticles, J. Transl. Med. 15 (2017), 18, https://doi.org/10.1186/s12967-016-1115-2.

[30] H. Lian, J. Wu, Y. Hu, H. Guo, Self-assembled albumin nanoparticles for combination therapy in prostate cancer, Int. J. Nanomed. 12 (2017) 7777–7787.

[31] M.P. Wolf, et al., FRET in a polymeric nanocarrier: IR-780 and IR-780-PDMS, Biomacromolecules 11 (2019) 4065–4074.

[32] C. Yue, P. Liu, M. Zheng, P. Zhao, Y. Wang, Y. Ma, L. Cai, IR-780 dye loaded tumor targeting theranostic nanoparticles for NIR imaging and photothermal therapy, Biomaterials 34 (28) (2013) 6853–6861.

[33] C. Liang, A.Y. Park, J. Guan, In vitro scratch assay: a convenient and inexpensive method for analysis of cell migration in vitro, Nat. Protoc. 2 (2) (2007) 329–333.

[34] X. Zhao, Z. Fan, Y. Qiao, Y. Chen, S. Wang, X. Yue, T. Shen, W. Liu, J. Yang, H. Gao, X. Zhan, L. Shang, Y. Yin, W. Zhao, D. Ding, R. Xi, M. Meng, AIEgens conjugation improves the photothermal efficacy and near-infrared imaging of heptamethine cyanine IR-780, ACS Appl. Mater. Interfaces 12 (2020) 16114–16124, https://doi.org/10.1021/acsami.0c01715.

[35] W.B. Liechty, N.A. Peppas, Expert opinion: responsive polymer nanoparticles in cancer therapy, Eur. J. Pharm. Biopharm. 80 (2) (2012) 241–246.

[36] Y. Chen, Z. Li, H. Wang, Y. Wang, H. Han, Q. Jin, J. Ji, IR-780 loaded phospholipid mimicking homopolymeric micelles for near-IR imaging and photothermal therapy of pancreatic cancer, ACS Appl. Mater. Interfaces 8 (11) (2016) 6852–6858.

[37] T. Lin, A. Yuan, X. Zhao, H. Lian, J. Zhuang, W. Chen, Q. Zhang, G. Liu, S. Zhang, W. Chen, W. Cao, C. Zhang, J. Wu, Y. Hu, H. Guo, Self-assembled tumor-targeting hyaluronic acid nanoparticles for photothermal ablation in orthotopic bladder cancer, Acta Biomater. 53 (2017) 427–438.

[38] Y. Cheng, H. Cheng, C. Jiang, X. Qiu, K. Wang, W. Huan, A. Yuan, J. Wu, Y. Hu, Perfluorocarbon nanoparticles enhance reactive oxygen levels and tumour growth inhibition in photodynamic therapy, Nat. Commun. 6 (1–8) (2015) 8785, https://doi.org/10.1038/ncomms9785.

[39] T.H. Tran, H.T. Nguyen, T.T. Phuong Tran, S.K. Ku, J.H. Jeong, H.G. Choi, C. S. Yong, J.O. Kim, Combined photothermal and photodynamic therapy by hyaluronic acid- decorated polypyrrole nanoparticles, Nanomedicine 12 (2017) 1511–1523, https://doi.org/10.2217/nnm-2016-0438.

[40] I.R. Calori, H. Bi, A.C. Tedesco, Expanding the limits of photodynamic therapy: the design of organelles and hypoxia-targeting nanomaterials for enhanced photokilling of cancer, ACS Appl. Bio Mater. 4 (2021) 195–228, https://doi.org/10.1021/acsabm.0c00945.

[41] I.R. Calori, A.C. Tedesco, Aluminum chloride phthalocyanine in MCF-7: rationally accounting for state of aggregation of photosensitizers inside cells, Dyes Pigments 173 (2020), 107940.

[42] J.L. Guerriero, D. Ditsworth, Y. Fan, F. Zhao, H.C. Crawford, W.X. Zong, Chemotherapy induces tumor clearance independent of apoptosis, Cancer Res. 68 (23) (2008) 9595–9601, https://doi.org/10.1158/0008-5472.CAN-08-2452.

[43] A.C. Gasparovic, L. Milkovic, S.B. Sunjic, N. Zarkovic, Cancer growth regulation by 4-hydroxynonenal, Free Radic. Biol. Med. 111 (2017) 226–234.

[44] V.C.F. Mosqueira, P. Legrand, R. Gref, B. Heurtault, M. Appel, G. Barratt, Interactions between a macrophage cell line (J774A1) and surface-modified poly (D,L-lactide) nanocapsules bearing poly(ethylene glycol), J. Drug Target. 7 (1) (1999) 65–78, https://doi.org/10.3109/10611869909085493.

[45] I.C. Trindade, G. Pound-Lana, D.G.S. Pereira, L. de Oliveira, M.S. Andrade, J.M. C. Vilela, B.B. Postacchini, V.C.F. Mosqueira, Mechanisms of interaction of biodegradable polyester nanocapsules with non-phagocytic cells, Eur. J. Pharm. Sci. 124 (2018) 89–104, https://doi.org/10.1016/j.ejps.2018.08.024.

[46] A.S. Levenson, C. Jordan, MCF-7: the first hormone-responsive breast cancer cell line, Perspect. Cancer Res. 57 (57) (1997) 3071–3079.

[47] D. Flodrova, L. Toporova, D. Macejova, M. Lastovickova, J. Brtko, J. Bobalova, A comparative study of protein patterns of human estrogen receptor positive (MCF-7) and negative (MDA-MB-231) breast cancer cell lines, Gen. Physion. Biophys. 35 (2016) 387–392.

[48] Y. Hashimoto, S. Tatsumi, R. Takeda, A. Naka, N. Ogane, Y. Kameda, K. Kawachi, S. Shimizu, M. Sakai, S. Kamoshida, Expression of organic anion-transporting polypeptide 1A2 and organic cation transporter 6 as a predictor of pathologic response to neoadjuvant chemotherapy in triple negative breast cancer, Breast Cancer Res. Treat. 145 (2014) 101–111.

[49] N. Banerjee, H. Fonge, A. Mikhail, R.M. Reilly, R. Bendayan, C. Allen, Estrone-3-sulphate, a potential novel ligand for targeting breast cancers, PLoS One 8 (5) (2013) 2–10, https://doi.org/10.1371/journal.pone.0064069.

[50] H. Hillaireau, P. Couvreur, Nanocarriers' entry into the cell: relevance to drug delivery, Cell. Mol. Life Sci. 66 (17) (2009) 2873–2896, https://doi.org/10.1007/s00018-009-0053-z.

[51] J.M. Rabanel, V. Aoun, I. Elkin, M. Mokhtar, P. Hildgen, Drug-loaded nanocarriers: passive targeting and crossing of biological barriers, Curr. Med. Chem. 19 (2012) 3070–3102.

[52] X. Wang, Y. Qiu, M. Wang, C. Zhang, T. Zhang, H. Zhou, W. Zhao, W. Zhao, G. Xia, R. Shao, Endocytosis and organelle targeting of nanomedicines in cancer therapy, Int. J. Nanomed. 15 (2020) 9447–9467.